

# SURFACTANT-DEPENDENT CONTACT LINE DYNAMICS AND DROPLET ADHESION ON TEXTURED SUBSTRATES: DERIVATIONS AND COMPUTATIONS

YUAN GAO

*Department of Mathematics, Duke University, Durham, NC*

JIAN-GUO LIU

*Department of Mathematics and Department of Physics, Duke University, Durham, NC*

**ABSTRACT.** We study the adhesion of a droplet with insoluble surfactant laid on its capillary surface to a textured substrate. In this process, the surfactant-dependent surface tension dominates the behaviors of the whole dynamics, particularly the moving contact lines. This allows us to derive the full dynamics of the droplets laid by the insoluble surfactant: (i) the moving contact lines, (ii) the evolution of the capillary surface, and (iii) the surfactant dynamics on this moving surface with a boundary condition at the contact lines. Our derivations base on Onsager's principle with Rayleigh dissipation functionals for either the viscous flow inside droplets or the motion by mean curvature of the capillary surface. We also prove the Rayleigh dissipation functional for the viscous flow case is stronger than the one for the motion by mean curvature. After incorporating the textured substrate profile, we design numerical schemes based on unconditionally stable explicit boundary updates and moving grids, which enable efficient computations for many challenging examples showing the significant contributions of the surfactant.

## 1. INTRODUCTION

The dynamics of droplets adhering to an impermeable substrate is not only a fundamental mathematical problem but also has a wide range of practical applications such as droplet-based microfluidics in drug discovery, sensor design and enhanced oil recovery [23, 3, 22]. Particularly, the addition of surfactant (i.e. surface-active agent) can significantly change the effective surface tension of the capillary surface, and thus dominates the dynamics of droplets. Therefore, mathematical derivations, validations and numerical simulations for dynamics of a droplet laid by insoluble surfactant coupled with moving contact lines are important and demanding topics; see [4, 19, 18, 30].

---

*E-mail addresses:* yuangao@math.duke.edu, jliu@math.duke.edu.

*Date:* November 27, 2021.

*Key words and phrases.* Onsager reciprocal relations, dynamic surface tension, dynamic contact angles, Marangoni flow, Stokes flow.

First, the adhering process of a small droplet placed on an impermeable textured substrate is mainly driven by the capillary effect. That is to say, the droplet tends to minimize the surface energy  $\mathcal{F}$ , which consists of the surface energy of three interfaces, denoted as  $\gamma_{\text{SL}}$  ( $\gamma_{\text{SG}}$  resp.) for solid-liquid interfaces (solid-gas resp.) and as  $\gamma_0$  for the liquid-gas interface without surfactant. Now we suppose there are insoluble surfactant (known as Langmuir monolayer) concentrating on the evolutionary capillary surface, i.e., the interface between the liquid inside the droplet and the gas surrounding it. With the surfactant, the surface energy density on the capillary surface will depend on the surface concentration of surfactant  $c$  and will be denoted as  $e(c)$ . During the adhering process, change of the surface concentration of surfactant  $c(\cdot, t)$  is induced by stretching and evolution of the capillary surface and the surfactant also has its own convection and diffusion on the capillary surface. More importantly, the concentration-dependent surface tension  $\gamma(c)$ , with the unit force/length, has the same unit with the energy density  $e(c)$  (energy/area) but no longer equals  $e(c)$ . The relation between the concentration-dependent surface tension  $\gamma(c)$  and the free energy density  $e(c)$  of the surfactant-covered capillary surface is given by  $\gamma(c) = e(c) - e'(c)c$ ; see [7, 13] and derivations in Section 2.3 below. Therefore, the concentration-dependent surface tension  $\gamma(c)$  will in turn significantly alter the motion of the capillary surface and moving contact lines, i.e., the lines where three phases (liquid, gas and solid) meet. This fundamental question on surfactant effect for the contact line dynamics of droplets was discussed in the review article [4] by DE GENNES. There are many recent theoretical and numerical studies on this subject, including insoluble or soluble surfactant; c.f. [13, 19, 18, 16, 30, 27, 2, 9, 29, 17, 10, 26, 8] and the references therein.

Since the surfactant-dependent capillary effect dominates the whole adhesion process, we regard the geometric states, including wetting domain  $\Omega_t$  and capillary surface  $h(x, y, t)$ , as the configurations for the droplet dynamics. We will first derive the dynamics of the surfactant moving with the capillary surface represented by a graph function  $h(x, y, t)$  with some proper boundary conditions at the contact lines. Then combining the total energy  $\mathcal{F}$  defined in (2.46), a Rayleigh dissipation functional defined in (2.47) and Onsager's principle [7, 8], we derive the governing equations for the whole system. As explained below, we focus on how the surfactant-dependent surface tension  $\gamma(c)$  naturally appears in the whole system.

First, we observe the motion of the capillary surface is driven by the concentration-dependent force  $\gamma(c)H$  per unit area (known as the Laplace pressure), where  $H$  is the mean curvature of the capillary surface. This observation mainly relies on the energy law (2.28) for the capillary surface. Second, the most complicated competition, relaxation and balance happen at the contact lines, so we need to derive a concentration-dependent unbalanced Young force at the contact lines. Without the surfactant, the unbalanced Young force [4] at the contact lines is

$$F_Y = \gamma_{\text{SG}} - \gamma_{\text{SL}} - \gamma_0 \cos \theta_{\text{CL}} = \gamma_0 (\cos \theta_Y - \cos \theta_{\text{CL}}), \quad \cos \theta_Y := \frac{\gamma_{\text{SG}} - \gamma_{\text{SL}}}{\gamma_0},$$

where  $\theta_{\text{CL}}$  is the dynamic contact angle, i.e., the angle (inside the droplet) between capillary surface and the solid substrate; see Fig. 1. Then with a dissipation mechanism, Onsager's linear response theory with friction coefficient  $\xi$ , one can obtain the relation between the contact line speed  $v_{\text{CL}}$  and this driven force, and thus obtain the dynamics of the moving contact lines  $\xi v_{\text{CL}} = F$ . However, with the presence of the surfactant, how does the surfactant transport and how does the energy

exchanges at the moving contact lines are challenging questions. We will first derive a Robin-type boundary condition (2.39) of the surfactant dynamics at the moving contact lines, which is consistent with both the mass conservation law and the energy conservation law; see Section 2.4. Then we adapt this boundary condition to derive the concentration-dependent unbalanced Young force at the contact lines

$$(1.1) \quad F_s = \gamma_{SG} - \gamma_{SL} - \gamma(c) \cos \theta_{CL},$$

in which the concentration-dependent surface tension is exactly the one  $\gamma(c) = e(c) - e'(c)c$ . Hence the dynamics of the moving contact line with the surfactant effect is

$$(1.2) \quad \xi v_{CL} = F_s.$$

We refer to (4.16) for the corresponding effective Young force after including a textured substrate.

In summary, the full adhering process of the droplets can be described by (i) the transport of the surfactant, (ii) the moving contact lines and (iii) the evolution of the capillary surface; see (2.50) for 3D droplets with a volume constraint and see (4.16) for 2D droplets placed on a textured substrate including the gravitational effect. Our derivations for the geometric motion of droplets, basing on a graph representation  $h(x, y, t)$  of the capillary surface, also enable us to design an unconditionally stable and efficient numerical scheme; see Section 4.

If we further consider the surfactant-induced Marangoni flow inside the droplets, the derivations for the purely geometric motion in Section 2 can be easily adapted to the bulk viscous flow based on Onsager's principle. In this case, there is an additional convention of the surfactant on the capillary surface contributed from the bulk fluid velocity. This convention, together with the gradient of the concentration-dependent surface tension  $\nabla \gamma(c)$ , leads to the Marangoni flow. Then the Robin-type boundary condition (2.39) for  $c$  at the contact lines becomes no-flux boundary condition (3.10), which is also used in [30]. With the additional Marangoni stress, after incorporating the transport equation for the surfactant, Onsager's principle immediately yields the corresponding governing equations (3.18) for the surfactant-induced Marangoni flow model for droplets on a substrate; see details in Section 3. We also show the Onsager reciprocal relations for both geometric motion case and the viscous flow case and in Proposition 3.1, we prove the dissipation functional for the viscous flow case is stronger than the one in the geometric motion model.

In Section 4, we propose a numerical scheme for the full dynamics of 2D droplets laid by the surfactant and placed on a textured substrate. This unconditionally stable scheme relies on the combination of the surfactant updates, which constantly change the effective surface tension  $\gamma(c)$ , and the splitting method with the 1st/2nd order accuracy that developed in [11] for the purely geometric motion of a single droplet without surfactant. Specifically, at each step, we first use unconditionally stable explicit updates for the moving contact lines, which efficiently decouple the computations for the motion of the capillary surface and the contact line dynamics. Then we adapt the arbitrary Lagrangian-Eulerian (ALE) method to handle the moving grids to update the profile of the capillary surface and the concentration of surfactant with the Robin-type boundary condition (4.10) at the contact lines. Based on this, some challenging examples showing significant effects of surfactant to the droplets dynamics will be conducted in Section 5. These include (i) the surface tension decreasing phenomena and asymmetric capillary surfaces due to the presence of the

surfactant; (ii) the enhanced rolling down for droplets placed on an inclined substrate; (iii) droplets on a textured substrate or a container with different surfactant concentrations.

The organization of this paper is as follows. In Section 2, we derive the geometric motion of 3D droplets, i.e., the moving contact lines, the evolution of the capillary surface and the surfactant dynamics on it, in which we incorporate the surfactant-dependent surface tension  $\gamma(c)$ . In Section 3, we derive the full dynamics of a 3D droplet with the surfactant-induced Marangoni flow inside it. In Section 4, we present the numerical schemes for 2D droplets placed on an inclined textured substrate based on the splitting method. In Section 5, we conduct some challenging examples showing the significant contributions of the surfactant to the whole adhering process.

## 2. DERIVATION FOR 3D CONTACT LINE DYNAMICS WITH SURFACTANT

We study the motion of a 3D droplet placed on a substrate, which is identified by the region  $A_t := \{(x, y, z); (x, y) \in \Omega_t, 0 \leq z \leq h(x, y, t)\}$  with a sharp interface. The motion of this droplet is described by a moving capillary surface  $S_t$ , and a partially wetting domain  $\Omega_t$  with free boundaries  $\partial\Omega_t$  (physically known as the contact lines); see Fig. 1(a). To clarify notations, let  $\Omega_t$  be a wetting domain, which is a simple connected 2D open set. Let  $h(x, y, t), (x, y) \in \Omega_t$  be the graph representation for the moving capillary surface. Then the capillary surface can be represented as

$$(2.1) \quad S_t := \{(x, y, h(x, y, t)), (x, y) \in \Omega_t\}.$$

Denote  $\gamma_{\text{SL}}$  ( $\gamma_{\text{SG}}$  resp.) as the interfacial surface energy density between solid-liquid phases (solid-gas resp.).  $\gamma_{\text{SL}}, \gamma_{\text{SG}}$  are constants but the interfacial surface energy on the capillary surface, i.e., the interface between liquid and gas, will depend on the insoluble surfactant on it. Denote  $c(x, y, t)$  as the surface concentration of the surfactant on the capillary surface, i.e., the number of the surfactant molecules per unit area. Let  $e(c)$  be the surface energy density on the capillary surface. Then the total surface energy of the droplet is

$$(2.2) \quad \mathcal{F}(h(x, y, t), \Omega_t, c(x, y, t)) := \int_{\Omega_t} e(c) \sqrt{1 + |\nabla h|^2} \, dx \, dy + (\gamma_{\text{SL}} - \gamma_{\text{SG}}) \int_{\Omega_t} dx \, dy.$$

We assume the following two constraints: the volume constraint  $V$  for the droplet and the total mass constraint  $M$  for the surfactant, i.e.

$$(2.3) \quad \int_{\Omega_t} h \, dx \, dy = V, \quad \int_{\Omega_t} c \sqrt{1 + |\nabla h|^2} \, dx = M.$$

Define the contact angles (the angle inside the droplet  $A$  between the capillary surface and the solid substrate) at contact lines  $\partial\Omega$  as  $\theta_{\text{CL}}$  such that

$$(2.4) \quad \tan \theta_{\text{CL}} = |\nabla h|.$$

We regard the geometric states, i.e., the wetting domain  $\Omega_t$  and the capillary surface  $h(x, y, t)$  as configurations of droplets. We assume the surfactant concentrates on the capillary surface, move with the evolutionary surface and may also has its own convection and diffusion on the surface. In the following subsections, we will first derive the continuity equation, the energy law and the boundary conditions for the concentration of the surfactant  $c$  on a prescribed moving capillary

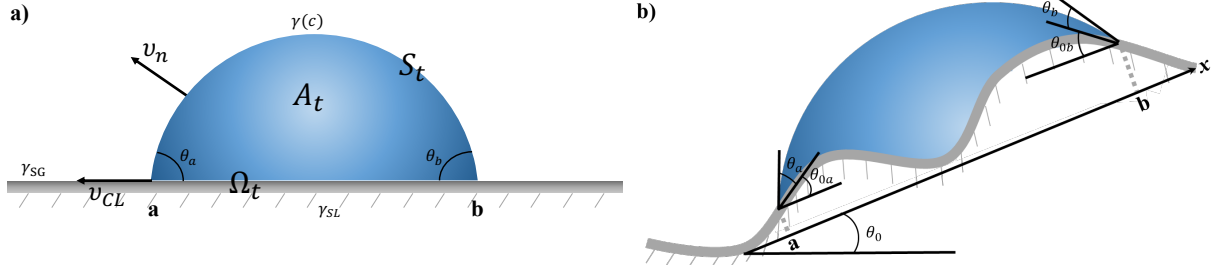


FIGURE 1. Illustration of surface tensions  $\gamma_{SG}$ ,  $\gamma_{SL}$ ,  $\gamma(c)$  on three interfaces, contact angle  $\theta_{CL}$ , capillary surface  $S_t$  and wetting domain  $\Omega_t$  for droplets on a plane (left) or on an inclined substrate with an effective inclined angle  $\theta_0$  (right).

surface  $h$ . Second, we calculate the energy dissipation law, and then using a specific Rayleigh dissipation functional and Onsager's principle, we derive the surfactant-dependent unbalanced Young force and finally the governing equations for the full dynamics of 3D droplets laid by the surfactant.

**2.1. The continuity equation for the surfactant represented in the  $xy$ -plane.** Surfactant dynamics on an evolutionary surface with the mass conservation law is a well-known model, c.f. [24]. For the case the surface has a graph representation  $h(x, y, t)$ , we will provide a simple derivation for the continuity equation for the concentration of the surfactant  $c(x, y, t)$ ,  $(x, y) \in \Omega_t$  on the capillary surface.

First, assume there is an underlying velocity field  $v \in \mathbb{R}^3$  driving the motion of the capillary surface and transporting the surfactant on the capillary surface, i.e., the normal component of velocity  $v$  shall agree with the normal velocity of the moving surface  $h$ . To clarify functions of  $(x, y)$  and functions of  $(x, y, z)$ , we introduce notations

$$(2.5) \quad \begin{aligned} v(x, y, z, t) &=: (v_x, v_y, v_z)(x, y, z, t), \\ v(x, y, z, t)|_{z=h(x, y, t)} &=: (v_1, v_2, v_3)(x, y, t). \end{aligned}$$

Therefore suppose

$$(2.6) \quad \begin{aligned} (v_1, v_2, v_3)(x, y, t) &= (v_n n + f\tau_1 + g\tau_2)(x, y, t), \\ n &:= \frac{1}{\sqrt{1 + |\nabla h|^2}}(-h_x, -h_y, 1), \quad \tau_1 := (1, 0, h_x), \quad \tau_2 := (0, 1, h_y), \quad v_n := \frac{h_t}{\sqrt{1 + |\nabla h|^2}} \end{aligned}$$

for some  $f(x, y, t), g(x, y, t)$ .

Second, we use the  $xy$ -component of velocity  $v$  to define a flow map on the  $xy$ -plane

$$(2.7) \quad \begin{cases} \dot{x} = v_1 = v_n n_1 + f = \frac{-h_x v_n}{\sqrt{1 + |\nabla h|^2}} + f, \\ \dot{y} = v_2 = v_n n_2 + g = \frac{-h_y v_n}{\sqrt{1 + |\nabla h|^2}} + g. \end{cases}$$

This flow map defines a moving 2D element  $\omega_t \subset \Omega_t$  via the pushforward  $\omega_t = (x(t), y(t))_{\#} \omega_0$  from any initial element  $\omega_0$ . In the absence of diffusion,  $\omega_t$  can be regarded as a material element.

Third, by the conservation of mass and the Reynolds transport theorem

$$(2.8) \quad 0 = \frac{d}{dt} \int_{\omega_t} c \sqrt{1 + |\nabla h|^2} \, dx \, dy = \int_{\omega_t} \partial_t (c \sqrt{1 + |\nabla h|^2}) + \nabla \cdot \left( c \sqrt{1 + |\nabla h|^2} \begin{pmatrix} v_1 \\ v_2 \end{pmatrix} \right) \, dx \, dy.$$

Then by the arbitrary of  $\omega_t$ , the continuity equation for  $c(x, y, t)$  is

$$(2.9) \quad \partial_t \left( c \sqrt{1 + |\nabla h|^2} \right) + \nabla \cdot \left( c \sqrt{1 + |\nabla h|^2} \begin{pmatrix} v_1 \\ v_2 \end{pmatrix} \right) = 0 \quad \text{in } \Omega_t.$$

Plugging  $v_1, v_2$  defined in (2.7), we obtain the continuity equation for  $c$

$$(2.10) \quad \begin{aligned} 0 &= \partial_t c \sqrt{1 + |\nabla h|^2} + \frac{c}{\sqrt{1 + |\nabla h|^2}} \nabla h \cdot \nabla h_t - \nabla \cdot \left( \frac{c h_t}{\sqrt{1 + |\nabla h|^2}} \nabla h \right) + \nabla \cdot \left( c \sqrt{1 + |\nabla h|^2} \begin{pmatrix} f \\ g \end{pmatrix} \right) \\ &= \partial_t c \sqrt{1 + |\nabla h|^2} - h_t \nabla \cdot \left( \frac{c}{\sqrt{1 + |\nabla h|^2}} \nabla h \right) + \nabla \cdot \left( c \sqrt{1 + |\nabla h|^2} \begin{pmatrix} f \\ g \end{pmatrix} \right) \end{aligned}$$

After simplification, the continuity equation for  $c$  is

$$(2.11) \quad \begin{aligned} 0 &= \partial_t c - v_n \nabla \cdot \left( \frac{c}{\sqrt{1 + |\nabla h|^2}} \nabla h \right) + \frac{1}{\sqrt{1 + |\nabla h|^2}} \nabla \cdot \left( c \sqrt{1 + |\nabla h|^2} \begin{pmatrix} f \\ g \end{pmatrix} \right) \\ &= \partial_t c - v_n \nabla c \cdot \frac{\nabla h}{\sqrt{1 + |\nabla h|^2}} - v_n c H + \frac{1}{\sqrt{1 + |\nabla h|^2}} \nabla \cdot \left( c \sqrt{1 + |\nabla h|^2} \begin{pmatrix} f \\ g \end{pmatrix} \right) \end{aligned}$$

for  $(x, y) \in \Omega_t$ , where  $H := \nabla \cdot \left( \frac{\nabla h}{\sqrt{1 + |\nabla h|^2}} \right)$  is the mean curvature.

2.1.1. *lift-up dynamics on the evolving capillary surface.* First, let

$$(2.12) \quad X(t) = (x(t), y(t), h(x(t), y(t), t)) \quad \text{for } (x(t), y(t)) \text{ satisfies (2.7)}$$

be a point on the moving surface  $S_t$ . Then one has

$$(2.13) \quad \dot{X} = (\dot{x}, \dot{y}, h_x \dot{x} + h_y \dot{y} + h_t) = v_n n + (f, g, h_x f + h_y g) = v.$$

Denote  $\mathcal{C}(x, y, z, t), (x, y, z) \in S_t$  as the surface concentration of surfactant on the capillary surface<sup>1</sup>. Then we have

$$(2.14) \quad \mathcal{C}(x, y, h(x, y, t), t) = c(x, y, t),$$

$$(2.15) \quad \frac{d}{dt} \mathcal{C}(x(t), y(t), h(x, y, t), t) = (\partial_t + v \cdot \nabla) \mathcal{C} = (\partial_t + v_1 \partial_x + v_2 \partial_y) c = \frac{d}{dt} c(x(t), y(t), t).$$

Then we have the following proposition on the equivalent formulation of the continuity equation in terms of  $\mathcal{C}$  defined on the moving surface  $S_t$ . The proof of this proposition will be given in Appendix A.

**Proposition 2.1.** *The continuity equation (2.9) can be recast as*

$$(2.16) \quad (\partial_t + v \cdot \nabla) \mathcal{C} + \mathcal{C} \nabla_s \cdot v_s - v_n \mathcal{C} H = 0 \quad \text{on } S_t,$$

where  $H = -\nabla_s \cdot n$  and  $\nabla_s$  is the surface divergence.

---

<sup>1</sup>We remark the standard notation in chemistry for the surface concentration is  $\Gamma$ .

*Remark 1.* By some elementary calculations, we remark (2.16) is equivalent to [13, (2.13)]

$$\begin{aligned}
 (2.17) \quad 0 &= \partial_t \mathcal{C} + v_n \cdot \nabla \mathcal{C} + v_s \cdot \nabla \mathcal{C} + \mathcal{C} \nabla_s \cdot v_s - v_n \mathcal{C} H \\
 &= \partial_t \mathcal{C} + v_n \cdot \nabla \mathcal{C} + \nabla_s \cdot (\mathcal{C} v_s) - v_n \mathcal{C} H \\
 &= \partial_t \mathcal{C} + v_n \cdot \nabla \mathcal{C} + \nabla_s \cdot (\mathcal{C} v),
 \end{aligned}$$

and is also equivalent to [18, (2.10)]

$$\begin{aligned}
 (2.18) \quad 0 &= \partial_t \mathcal{C} + v \cdot \nabla \mathcal{C} + \mathcal{C} \nabla_s \cdot v_s - v_n \mathcal{C} H \\
 &= (\partial_t + v \cdot \nabla) \mathcal{C} + \mathcal{C} \nabla_s \cdot v.
 \end{aligned}$$

Notice all these equivalent equations differ from ones presented in [24], and are only agree with [24] if the gradient of concentration  $\mathcal{C}$  is computed using the normally constant extension [1]. However, from [15],  $(\partial_t + v \cdot \nabla)$  is a tangential derivative of the space-time surface  $\cup_{t \geq 0} S_t \times \{t\}$ , so there is no need to extend  $\mathcal{C}$  outside the space-time surface.

In the case that there is no tangential velocity on the moving surface, i.e.,  $v_s = 0$ , the continuity equation becomes

$$\begin{aligned}
 (2.19) \quad 0 &= \partial_t c - v_n \nabla \cdot \left( \frac{c}{\sqrt{1 + |\nabla h|^2}} \nabla h \right) \\
 &= \partial_t c - v_n \nabla c \cdot \frac{\nabla h}{\sqrt{1 + |\nabla h|^2}} - v_n c H
 \end{aligned}$$

This formula is particularly efficient for simulating the purely geometric motion of the droplet and the surfactant is pinned and move with the capillary surface. For the case  $v_s \neq 0$ , one needs to consider the fluids inside the droplets instead of the purely geometric motion; see Section 3.

**2.2. Diffusion of surfactant on the evolutionary surface.** Furthermore, from some elementary calculations, the Dirichlet energy for the surfactant on the capillary surface is

$$(2.20) \quad \frac{1}{2} \int_{\Omega_t} |\nabla_s \mathcal{C}|^2 \sqrt{1 + |\nabla h|^2} \, dx \, dy = \frac{1}{2} \int_{\Omega_t} \frac{1}{\sqrt{1 + |\nabla h|^2}} \nabla c \cdot (M \nabla c) \, dx \, dy,$$

where  $M := I + \begin{pmatrix} -h_y \\ h_x \end{pmatrix} (-h_y, h_x)$ . Then the variation of the Dirichlet energy gives the Laplace–Beltrami operator in the graph representation,

$$\Delta_s c := \frac{1}{\sqrt{1 + |\nabla h|^2}} \nabla \cdot \left( \frac{1}{\sqrt{1 + |\nabla h|^2}} M \nabla \right) c.$$

Thus in the case of  $v_s = 0$ , the continuity equation (2.19) for the surfactant with additional diffusion becomes

$$(2.21) \quad c_t - \frac{h_t}{\sqrt{1 + |\nabla h|^2}} \nabla \cdot \left( \frac{c \nabla h}{\sqrt{1 + |\nabla h|^2}} \right) = D \Delta_s c,$$

which is equivalent to

$$(2.22) \quad \partial_t c - v_n \nabla c \cdot \frac{\nabla h}{\sqrt{1 + |\nabla h|^2}} - v_n c H = D \Delta_s c.$$

This is the continuity equation with diffusion for the surfactant dynamics on the moving surface and we will impose the no-flux boundary condition for (2.21) below. Another equivalent form of (2.21) in the conservative form is

$$(2.23) \quad \partial_t \left( c \sqrt{1 + |\nabla h|^2} \right) - \nabla \cdot \left( \frac{ch_t}{\sqrt{1 + |\nabla h|^2}} \nabla h \right) = D \nabla \cdot \left( \frac{1}{\sqrt{1 + |\nabla h|^2}} M \nabla \right) c.$$

**2.3. The energy law on the capillary surface.** In this section, given an evolutionary capillary surface  $h(x, y, t)$  and the associated surfactant dynamics (2.21) with (2.39), we calculate the energy law for the capillary surface.

Consider the free energy on the capillary surface

$$(2.24) \quad \mathcal{F}_0 = \int_{\Omega_t} e(c) \sqrt{1 + |\nabla h|^2} \, dx \, dy,$$

where  $e(c)$  is the energy density on the capillary surface and  $c(x, y, t)$  satisfies (2.21).

However, in calculations of the energy conservation law, the work done by the surface tension shall be a concentration-dependent one, given by  $\gamma(c)H$ , where  $\gamma(c)$  is the effective surface tension and  $H = \nabla \cdot \left( \frac{\nabla h}{\sqrt{1 + |\nabla h|^2}} \right)$  is the mean curvature. We will derive this energy conservation law below.

First, the relation between the concentration-dependent surface tension  $\gamma(c)$  with the free energy density  $e(c)$  is given by [7, 13]

$$(2.25) \quad \gamma(c) = e(c) - e'(c)c.$$

Indeed, from [7, (4.32)],  $\gamma(c) = \gamma_0 - \Pi_A(c)$ . Here  $\gamma_0 = e(0)$  and  $\Pi_A$  is the surface pressure which can be calculated by the osmotic pressure inside the interfacial layer due to the inhomogeneous surface concentration of surfactant. From the same derivations as [7, (2.16)],

$$\Pi_A(c) = -e(c) + e'(c)c + e_0.$$

Thus we have (2.25).

Second, multiplying (2.22) by  $e'(c)\sqrt{1 + |\nabla h|^2}$ , we have

$$\partial_t e(c) \sqrt{1 + |\nabla h|^2} - \nabla e(c) \cdot \frac{h_t \nabla h}{\sqrt{1 + |\nabla h|^2}} - h_t H e'(c)c = D \sqrt{1 + |\nabla h|^2} e'(c) \Delta_s c.$$

We can recast this in the conservative form

$$(2.26) \quad \begin{aligned} & \partial_t \left( e(c) \sqrt{1 + |\nabla h|^2} \right) - \nabla \cdot \left( e(c) \cdot \frac{h_t \nabla h}{\sqrt{1 + |\nabla h|^2}} \right) - h_t H e'(c)c \\ & - e(c) \partial_t \left( \sqrt{1 + |\nabla h|^2} \right) + e(c) \nabla \cdot \left( \frac{h_t \nabla h}{\sqrt{1 + |\nabla h|^2}} \right) = D \sqrt{1 + |\nabla h|^2} e'(c) \Delta_s c. \end{aligned}$$

Then using the identity

$$(2.27) \quad -\partial_t \left( \sqrt{1 + |\nabla h|^2} \right) + \nabla \cdot \left( \frac{h_t \nabla h}{\sqrt{1 + |\nabla h|^2}} \right) = h_t H$$

and relation (2.25), we simplify (2.26) as

$$(2.28) \quad \partial_t \left( e(c) \sqrt{1 + |\nabla h|^2} \right) - \nabla \cdot \left( e(c) \cdot \frac{h_t \nabla h}{\sqrt{1 + |\nabla h|^2}} \right) + \gamma(c) H h_t = D \sqrt{1 + |\nabla h|^2} e'(c) \Delta_s c.$$



The first term in (2.28) is the rate of change of the energy density per unit area in the  $xy$ -plane. The second term in (2.28) is the flux of energy density. The third term in (2.28), i.e.,  $\gamma(c)Hh_t = \gamma(c)Hv_n\sqrt{1+|\nabla h|^2}$  is the rate of work done by the surface tension per unit area in the  $xy$ -plane. The last term in (2.28) is the energy density dissipation due to the diffusion of the surfactant.

Now we focus on our goal to derive the contact line dynamics which is driven by the effective surface tension  $\gamma(c)$ . However, at the contact lines, we observe the horizontal velocity  $(v_1, v_2)$  defined by the flow map is *not* same as the contact line velocity. In the next subsection, we will discuss the correct boundary condition for the concentration of the surfactant.

The fundamental relation (2.25) implies the decreasing of  $\gamma(c)$  from the convexity of energy density  $e(c)$ . Many interesting physical phenomena can be explained by the decreasing of effective surface tension  $\gamma(c)$  due to the surfactant dynamics. We remark a typical  $\gamma$ , derived from the Langmuir equation, is given by

$$(2.29) \quad \gamma(c) = \gamma_0 + c_s kT \ln(1 - \frac{c}{c_s}), \quad e(c) = \gamma_0 + kT ((c_s - c) \ln(c_s - c) + c \ln c - c_s \ln c_s),$$

where  $\gamma_0$  is the surface tension without the surfactant and  $c_s$  is the saturated concentration [7]. We will demonstrate numerical examples using this typical  $\gamma$ .

**2.4. A boundary condition for the surfactant at the contact line.** To derive a boundary condition for the surfactant equation at the contact lines, we now apply the Reynolds transport theorem for the whole wetting domain  $\Omega_t$  upto its boundary. Notice the velocity of the contact lines is not the material velocity of the flow map (2.7) defined inside  $\Omega_t$ , we shall be careful when using the boundary velocity in the Reynolds transport theorem.

Denote  $n_\ell$  as the outer normal of the contact line  $\partial\Omega_t$  in the  $xy$ -plane and  $v_\ell$  as the velocity of the contact line. We have  $n_\ell = -\frac{\nabla h}{|\nabla h|}$  on the contact line  $\partial\Omega_t$ . Denote the normal speed of the contact line as  $v_{CL} := v_\ell \cdot n_\ell$ . By the Reynolds transport theorem we have

$$(2.30) \quad \frac{d}{dt} \int_{\Omega_t} c \sqrt{1+|\nabla h|^2} \, dx \, dy = \int_{\Omega_t} \partial_t \left( c \sqrt{1+|\nabla h|^2} \right) \, dx \, dy + \int_{\partial\Omega_t} c \sqrt{1+|\nabla h|^2} v_\ell \cdot n_\ell \, ds.$$

Then by (2.23) and integration by parts, we obtain

$$(2.31) \quad \int_{\Omega_t} \partial_t \left( c \sqrt{1+|\nabla h|^2} \right) \, dx \, dy = D \int_{\partial\Omega_t} \frac{1}{\sqrt{1+|\nabla h|^2}} M \nabla c \cdot n_\ell \, ds + \int_{\partial\Omega_t} \frac{ch_t}{\sqrt{1+|\nabla h|^2}} \nabla h \cdot n_\ell \, ds$$

Notice the definition of  $M$  gives

$$(2.32) \quad M \nabla c \cdot n_\ell = n_\ell \cdot \nabla c + n_\ell \cdot (-h_y, h_x) (-h_y, h_x) \cdot \nabla c = n_\ell \cdot \nabla c \quad \text{on } \partial\Omega_t.$$

Notice also the compatibility condition  $\frac{dh(x(t), y(t), t)}{dt} = 0$  on the contact line gives

$$(2.33) \quad h_t = -\nabla h \cdot v_\ell.$$

Then from  $n_\ell = -\frac{\nabla h}{|\nabla h|}$  on  $\partial\Omega_t$ , (2.33) becomes

$$(2.34) \quad h_t = |\nabla h| n_\ell \cdot v_\ell = |\nabla h| v_{CL},$$

which implies

$$(2.35) \quad \frac{h_t}{\sqrt{1+|\nabla h|^2}} \nabla h \cdot n_\ell = -\frac{|\nabla h|^2}{\sqrt{1+|\nabla h|^2}} v_{\text{CL}}.$$

Thus (2.31) can be further simplified as

$$(2.36) \quad \int_{\Omega_t} \partial_t \left( c \sqrt{1+|\nabla h|^2} \right) dx dy = \int_{\partial\Omega_t} D \frac{n_\ell \cdot \nabla c}{\sqrt{1+|\nabla h|^2}} - c \frac{|\nabla h|^2}{\sqrt{1+|\nabla h|^2}} v_{\text{CL}} ds.$$

Plugging this into (2.30), we have

$$(2.37) \quad \begin{aligned} & \frac{d}{dt} \int_{\Omega_t} c \sqrt{1+|\nabla h|^2} dx dy \\ &= \int_{\partial\Omega_t} \frac{D}{\sqrt{1+|\nabla h|^2}} n_\ell \cdot \nabla c - \int_{\partial\Omega_t} c \frac{|\nabla h|^2}{\sqrt{1+|\nabla h|^2}} v_{\text{CL}} - c \sqrt{1+|\nabla h|^2} v_{\text{CL}} ds \\ &= \int_{\partial\Omega_t} \frac{D}{\sqrt{1+|\nabla h|^2}} n_\ell \cdot \nabla c + \int_{\partial\Omega_t} c \frac{1}{\sqrt{1+|\nabla h|^2}} v_{\text{CL}} ds. \end{aligned}$$

Therefore, in order to maintain the mass conservation law

$$(2.38) \quad 0 = \frac{d}{dt} \int_{\Omega_t} c \sqrt{1+|\nabla h|^2} dx dy = \int_{\partial\Omega_t} \frac{1}{\sqrt{1+|\nabla h|^2}} (D n_\ell \cdot \nabla c + c v_{\text{CL}}) ds,$$

we impose the following Robin boundary condition for (2.21)

$$(2.39) \quad D n_\ell \cdot \nabla c + c v_{\text{CL}} = 0 \quad \text{on } \partial\Omega_t.$$

**2.5. Dissipation of the surface energy.** Using the Reynolds transport theorem for the surface energy

$$(2.40) \quad \begin{aligned} & \frac{d}{dt} \int_{\Omega_t} e(c) \sqrt{1+|\nabla h|^2} dx dy \\ &= \int_{\Omega_t} \partial_t \left( e(c) \sqrt{1+|\nabla h|^2} \right) dx dy + \int_{\partial\Omega_t} e(c) \sqrt{1+|\nabla h|^2} v_{\text{CL}} ds \\ &= \int_{\Omega_t} \nabla \cdot \left( e(c) \cdot \frac{h_t \nabla h}{\sqrt{1+|\nabla h|^2}} \right) - \gamma(c) H h_t + D e'(c) \nabla \cdot \left( \frac{1}{\sqrt{1+|\nabla h|^2}} M \nabla c \right) dx dy \\ & \quad + \int_{\partial\Omega_t} e(c) \sqrt{1+|\nabla h|^2} v_{\text{CL}} ds, \end{aligned}$$

where we used (2.28) in the last equality. Then using the integration by parts, (2.40) becomes

$$(2.41) \quad \begin{aligned} & \frac{d}{dt} \int_{\Omega_t} e(c) \sqrt{1+|\nabla h|^2} dx dy \\ &= \int_{\Omega_t} -h_t H \gamma(c) - D \frac{e''(c)}{\sqrt{1+|\nabla h|^2}} \nabla c \cdot M \nabla c dx dy \\ & \quad + \int_{\partial\Omega_t} e(c) \frac{h_t}{\sqrt{1+|\nabla h|^2}} \nabla h \cdot n_\ell + D e'(c) \frac{M \nabla c \cdot n_\ell}{\sqrt{1+|\nabla h|^2}} ds + \int_{\partial\Omega_t} e(c) \sqrt{1+|\nabla h|^2} v_{\text{CL}} ds. \end{aligned}$$

Then using (2.35) and (2.32), by the same calculations as (2.37), we have

$$(2.42) \quad \begin{aligned} & \frac{d}{dt} \int_{\Omega_t} e(c) \sqrt{1 + |\nabla h|^2} \, dx \, dy \\ &= \int_{\Omega_t} -h_t \gamma(c) H - D \frac{e''(c)}{\sqrt{1 + |\nabla h|^2}} \nabla c \cdot M \nabla c \, dx \, dy + \int_{\partial\Omega_t} \frac{1}{\sqrt{1 + |\nabla h|^2}} [De'(c) n_\ell \cdot \nabla c + e(c) v_{CL}] \, ds, \end{aligned}$$

From the boundary condition (2.39), we have

$$(2.43) \quad De'(c) n_\ell \cdot \nabla c + e(c) v_{CL} = -e'(c) c v_{CL} + e(c) v_{CL} = \gamma(c) v_{CL}.$$

Thus, this, together with (2.42), implies the dissipation of the surface energy  $\mathcal{F}_0$

$$(2.44) \quad \begin{aligned} & \frac{d}{dt} \int_{\Omega_t} e(c) \sqrt{1 + |\nabla h|^2} \, dx \, dy \\ &= \int_{\Omega_t} -\gamma(c) h_t H - D \frac{e''(c)}{\sqrt{1 + |\nabla h|^2}} \nabla c \cdot M \nabla c \, dx \, dy + \int_{\partial\Omega_t} \gamma(c) \cos \theta_{CL} v_{CL} \, ds, \end{aligned}$$

where we used  $\cos \theta_{CL} = \frac{1}{\sqrt{1 + |\nabla h|^2}}$  on  $\partial\Omega_t$ .

From (2.44) and the rate of change of the surface energy for the bottom part

$$\frac{d}{dt} (\gamma_{SL} - \gamma_{SG}) \int_{\Omega_t} dx \, dy = (\gamma_{SL} - \gamma_{SG}) \int_{\partial\Omega_t} v_{CL} \, ds,$$

we finally obtain the dissipation law of the surface energy

$$(2.45) \quad \begin{aligned} & \frac{d}{dt} \left( \int_{\Omega_t} e(c) \sqrt{1 + |\nabla h|^2} \, dx \, dy + (\gamma_{SL} - \gamma_{SG}) \int_{\Omega_t} dx \, dy \right) \\ &= \int_{\Omega_t} -\gamma(c) h_t H - D \frac{e''(c)}{\sqrt{1 + |\nabla h|^2}} \nabla c \cdot M \nabla c \, dx \, dy + \int_{\partial\Omega_t} (\gamma(c) \cos \theta_{CL} + \gamma_{SL} - \gamma_{SG}) v_{CL} \, ds. \end{aligned}$$

**2.6. The Onsager principle and the governing equations in 3D.** We take the total free energy of the droplet with volume constraint  $V$  as

$$(2.46) \quad \mathcal{F}(h(t), \Omega_t, \lambda(t)) = \int_{\Omega_t} e(c) \sqrt{1 + |\nabla u|^2} \, dx \, dy + (\gamma_{SL} - \gamma_{SG}) \int_{\Omega_t} dx \, dy - \lambda(t) \left( \int_{\Omega_t} h \, dx \, dy - V \right),$$

where  $\lambda(t)$  is a Lagrangian multiplier. Thus we have

$$\begin{aligned} \frac{d}{dt} \mathcal{F} &= - \int_{\Omega_t} (\gamma(c) H + \lambda) h_t \, dx \, dy - D \int_{\Omega_t} \frac{e''(c)}{\sqrt{1 + |\nabla h|^2}} \nabla c \cdot M \nabla c \, dx \, dy \\ &\quad + \int_{\partial\Omega_t} (\gamma(c) \cos \theta_{CL} + (\gamma_{SL} - \gamma_{SG})) v_{CL} \, ds. \end{aligned}$$

The derivation with some additional potential forces is standard and will not be included here.

We choose the Rayleigh dissipation functional as

$$(2.47) \quad Q(h_t, v_{CL}; h, c) := \frac{\beta}{2} \int_{\Omega_t} \frac{h_t^2}{\sqrt{1 + |\nabla h|^2}} \, dx \, dy + \frac{\xi}{2} \int_{\partial\Omega_t} |v_{CL}|^2 \, ds + \frac{D}{2} \int_{\Omega_t} \frac{e''(c)}{\sqrt{1 + |\nabla h|^2}} \nabla c \cdot M \nabla c \, dx \, dy,$$

where  $\beta$  represents the friction coefficient for the normal motion of the capillary surface,  $\xi$  represents the friction coefficient for the moving contact lines and the last term represents the dissipation due

to the diffusion of the surfactant. We will see the first term in (2.47) leads to the motion by mean curvature of the capillary surface [14]. Then minimizing the Rayleighian [7]

$$(2.48) \quad \mathcal{R}(h_t, v_{\text{CL}}; h, c) := Q(h_t, v_{\text{CL}}; h, c) + \frac{d}{dt} \mathcal{F}(h_t, v_{\text{CL}}; h, c)$$

with respect to  $(h_t, v_{\text{CL}})$  gives the governing equation

$$(2.49) \quad \begin{aligned} \frac{\beta}{\sqrt{1 + |\nabla h|^2}} h_t &= \gamma(c)H + \lambda, \\ \xi v_{\text{CL}} &= -\gamma(c) \cos \theta_{\text{CL}} - (\gamma_{\text{SL}} - \gamma_{\text{SG}}), \end{aligned}$$

where the right hand side  $F_s = -\gamma(c) \cos \theta_{\text{CL}} - (\gamma_{\text{SL}} - \gamma_{\text{SG}})$  is exactly the concentration-dependent unbalanced Young force.

Combining this with (2.21), the full system is

$$(2.50) \quad \begin{cases} \frac{\beta}{\sqrt{1 + |\nabla h|^2}} h_t = \gamma(c)H + \lambda, & h(x, y)|_{\partial\Omega_t} = 0, \\ c_t - \frac{h_t}{\sqrt{1 + |\nabla h|^2}} \nabla \cdot \left( \frac{c \nabla h}{\sqrt{1 + |\nabla h|^2}} \right) = D \Delta_s c, & cv_{\text{CL}} + D n_\ell \cdot \nabla c|_{\partial\Omega_t} = 0, \\ \xi v_{\text{CL}} = -\gamma(c) \cos \theta_{\text{CL}} - (\gamma_{\text{SL}} - \gamma_{\text{SG}}), & \text{on } \partial\Omega_t, \\ \int_{\Omega_t} h \, dx \, dy = V. \end{cases}$$

This system can be regarded as (i) the linear response relation of  $v_n$  to the Laplace pressure  $\gamma(c)H$ , (ii) the linear response relation of  $v_{\text{CL}}$  to the concentration-dependent unbalanced Young force  $F_s$ , and (iii) the transport of the insoluble surfactant on the capillary surface.

As a consequence, the energy dissipation relation is

$$(2.51) \quad \begin{aligned} \frac{d}{dt} \mathcal{F} &= - \int_{\Omega_t} \frac{\beta h_t^2}{\sqrt{1 + |\nabla h|^2}} \, dx \, dy - D \int_{\Omega_t} \frac{e''(c)}{\sqrt{1 + |\nabla h|^2}} \nabla c \cdot M \nabla c \, dx \, dy - \int_{\partial\Omega_t} \xi |v_{\text{CL}}|^2 \, ds \\ &= -2Q. \end{aligned}$$

In physics,  $\frac{2Q}{T}$  is denoted as  $\dot{S}$ , the entropy production rate.

We point out that the first dissipation term in Rayleigh dissipation functional (2.47) is not a standard one. Instead, the standard dissipation functional includes the dissipation due to the viscosity of fluids inside the droplet, for which we will also give a simple derivation using Onsager's principle in Section 3. However, our choice of the Rayleigh dissipation functional (2.47) allows us to study the purely geometric motion of the droplets and has the following advantages. (i) For small droplets, it captures the essential physics and the leading behaviors of the droplet dynamics; (ii) it satisfies the Onsager principle in physics and thus has the gradient flow structure so that this simplified model is friendly for theoretical studies; (iii) this model is also computationally efficient because it does not need to compute the fluids inside the droplets and the numerical schemes can be easily adapt to more complicated physical examples such as inclined textured substrates, the electrowetting and the surfactant dynamics considered here.

### 3. SURFACTANT-INDUCED MARANGONI STRESS AND VISCOUS FLOW

In this section, we derive the surfactant-induced Marangoni flow for droplets on a substrate by including the viscous bulk fluids inside the droplets. Including the fluid viscosity dissipation in the Rayleigh dissipation functional, instead of the first term in (2.47), will lead to the Stokes equations for fluids inside droplets [16, 30, 17] or the thin film equation in the lubrication approximation [17, 28]. Although different forms of viscous flow models coupled with moving contact lines and surfactant transport were derived previously, we adapt the energy law on the capillary surface (2.28) to the case  $v_s \neq 0$  and use Onsager's principle to give a simple derivation for the viscous bulk fluids inside the droplet with the Marangoni flow induced by the surfactant. At the end of this section, we also point out the two cases with or without bulk fluids inside the droplet are indeed quite similar in terms of the linear response relation  $u = \mathcal{K}F$ ; see (3.27). In Proposition 3.1, we will prove the Rayleigh dissipation functional for the viscous flow case is indeed stronger than the one for the motion by mean curvature of the capillary surface. However, for the bulk fluids cases with both the hydrodynamic effect and the surfactant effect, the computational strategies presented in Section 4 shall be modified and will be left as a future research.

Now we consider the case  $v_s \neq 0$ , i.e., the tangential velocity of the surfactant is determined by the fluids inside the droplet. For this case, the transport equation (2.23) for  $c$  becomes

$$(3.1) \quad \partial_t \left( c \sqrt{1 + |\nabla h|^2} \right) - \nabla \cdot \left( \frac{ch_t}{\sqrt{1 + |\nabla h|^2}} \nabla h \right) + \nabla \cdot \left( c \sqrt{1 + |\nabla h|^2} \begin{pmatrix} f \\ g \end{pmatrix} \right) = D \nabla \cdot \left( \frac{1}{\sqrt{1 + |\nabla h|^2}} M \nabla \right) c.$$

In the following subsections, we will adapt the same calculations as in Section 2 to the case  $v_s \neq 0$  and derive the energy law, the corresponding boundary conditions of the surfactant at the contact line, and then Onsager's principle immediately yields the governing equations for the bulk fluids coupled with transport of surfactant on the evolutionary surface.

**3.1. Energy law with the convection contribution.** Recall  $(v_1, v_2)(x, y, t)$  is the  $xy$ -component of the velocity of the moving capillary surface. Then (3.1) is recast as

$$(3.2) \quad \partial_t \left( c \sqrt{1 + |\nabla h|^2} \right) + \nabla \cdot \left( c \sqrt{1 + |\nabla h|^2} \begin{pmatrix} v_1 \\ v_2 \end{pmatrix} \right) = D \nabla \cdot \left( \frac{1}{\sqrt{1 + |\nabla h|^2}} M \nabla \right) c.$$

Then by same calculations as (2.28), we obtain the energy law

$$(3.3) \quad \begin{aligned} & \partial_t \left( e(c) \sqrt{1 + |\nabla h|^2} \right) + \nabla \cdot \left( e(c) \sqrt{1 + |\nabla h|^2} \begin{pmatrix} v_1 \\ v_2 \end{pmatrix} \right) \\ &= \gamma(c) \left( \partial_t \sqrt{1 + |\nabla h|^2} + \nabla \cdot \left( \sqrt{1 + |\nabla h|^2} \begin{pmatrix} v_1 \\ v_2 \end{pmatrix} \right) \right) + D \sqrt{1 + |\nabla h|^2} e'(c) \Delta_s c \\ &=: \gamma(c) I + D \sqrt{1 + |\nabla h|^2} e'(c) \Delta_s c. \end{aligned}$$

Here using the identity (2.27),  $\gamma(c)I$  can be further simplified as

$$\begin{aligned}\gamma(c)I &= -\gamma(c)h_t H - \nabla\gamma(c) \cdot \left( \sqrt{1+|\nabla h|^2} \begin{pmatrix} f \\ g \end{pmatrix} \right) + \nabla \cdot \left( \gamma(c)\sqrt{1+|\nabla h|^2} \begin{pmatrix} f \\ g \end{pmatrix} \right) \\ &= -\sqrt{1+|\nabla h|^2} \left( \gamma(c)v_n H + \begin{pmatrix} f \\ g \end{pmatrix} \cdot \nabla\gamma(c) \right) + \nabla \cdot \left( \gamma(c)\sqrt{1+|\nabla h|^2} \begin{pmatrix} f \\ g \end{pmatrix} \right).\end{aligned}$$

We claim the first term in  $\gamma(c)I$  satisfies

$$(3.4) \quad \gamma(c)v_n H + \begin{pmatrix} f \\ g \end{pmatrix} \cdot \nabla_{xy}\gamma(c) = v \cdot F \quad \text{with } v = v_n n + v_s, \quad F := \gamma(c)Hn + \nabla_s \gamma(\mathcal{C}).$$

Here  $\nabla_s \gamma(\mathcal{C})$  is called the Marangoni stress so the total capillary force density  $F$  on the capillary surface consists of both the Laplace pressure and the Marangoni stress. Indeed, from the orthogonality, we have

$$(3.5) \quad v \cdot F = v_n \gamma(c)H + v_s \cdot \nabla_s \gamma(\mathcal{C}) \quad \text{on } z = h(x, y, t).$$

By the definition of  $v_s$  and surface gradient, the last term is

$$\begin{aligned}v_s \cdot \nabla_s \gamma(\mathcal{C}) &= (f\tau_1 + g\tau_2) \cdot [(I - n \otimes n)\nabla\gamma(\mathcal{C})] \\ &= (f\tau_1 + g\tau_2) \cdot \nabla\gamma(\mathcal{C}) = \begin{pmatrix} f \\ g \end{pmatrix} \cdot \nabla_{xy}\gamma(c).\end{aligned}$$

**3.2. Boundary condition for the surfactant transport.** Using (3.2) and the same derivations as (2.37), we have

$$(3.6) \quad \begin{aligned}& \frac{d}{dt} \int_{\Omega_t} c \sqrt{1+|\nabla h|^2} \, dx \, dy \\ &= \int_{\partial\Omega_t} \frac{D}{\sqrt{1+|\nabla h|^2}} n_\ell \cdot \nabla c + \int_{\partial\Omega_t} c \frac{1}{\sqrt{1+|\nabla h|^2}} v_{\text{CL}} - c \sqrt{1+|\nabla h|^2} \begin{pmatrix} f \\ g \end{pmatrix} \cdot n_\ell \, ds.\end{aligned}$$

Recall (2.6) with  $v_s \neq 0$ . Suppose we impose the non-penetration boundary condition for the bulk fluid velocity  $v \cdot e_z|_{\partial\Omega_t} = 0$ . Then

$$(3.7) \quad v \cdot e_z = \frac{v_n}{\sqrt{1+|\nabla h|^2}} + h_x f + h_y g = 0 \quad \text{on } \partial\Omega_t.$$

Then by  $n_\ell = -\frac{\nabla h}{|\nabla h|}$ , we have

$$(3.8) \quad \frac{v_n}{\sqrt{1+|\nabla h|^2}} = |\nabla h| \begin{pmatrix} f \\ g \end{pmatrix} \cdot n_\ell.$$

From this and the continuity condition (2.34), we know the last two terms in (3.6) satisfy

$$(3.9) \quad \frac{1}{\sqrt{1+|\nabla h|^2}} v_{\text{CL}} - \sqrt{1+|\nabla h|^2} \begin{pmatrix} f \\ g \end{pmatrix} \cdot n_\ell = 0.$$

Therefore, for the case  $v_s \neq 0$ , under the non-penetration boundary condition  $v \cdot e_z|_{\partial\Omega_t} = 0$ , we naturally impose the no-flux boundary condition

$$(3.10) \quad n_\ell \cdot \nabla c|_{\partial\Omega_t} = 0$$

to ensure the conservation of mass. This no-flux boundary condition was used in [30], which used the Navier-Stokes equations to determine the fluid velocity  $v$ . Below, we focus on the Stokes flow model, which fit in the derivations using Onsager's principle very well.

**3.3. Rate of change of surface energy.** Using the energy law (3.3) and by the same calculations as (2.41), we have

$$\begin{aligned}
 (3.11) \quad & \frac{d}{dt} \int_{\Omega_t} e(c) \sqrt{1 + |\nabla h|^2} \, dx \, dy \\
 &= - \int_{\Omega_t} v \cdot F \sqrt{1 + |\nabla h|^2} \, dx \, dy - \int_{\Omega_t} D \frac{e''(c)}{\sqrt{1 + |\nabla h|^2}} \nabla c \cdot M \nabla c \, dx \, dy \\
 &+ \int_{\partial\Omega_t} e(c) \frac{h_t}{\sqrt{1 + |\nabla h|^2}} \nabla h \cdot n_\ell - ce'(c) \sqrt{1 + |\nabla h|^2} \begin{pmatrix} f \\ g \end{pmatrix} \cdot n_\ell \, ds + \int_{\partial\Omega_t} e(c) \sqrt{1 + |\nabla h|^2} v_{\text{CL}} \, ds,
 \end{aligned}$$

where we used the no-flux boundary condition (3.10). Using (3.9) and (2.35),

$$\begin{aligned}
 (3.12) \quad & \frac{d}{dt} \int_{\Omega_t} e(c) \sqrt{1 + |\nabla h|^2} \, dx \, dy \\
 &= - \int_{\Omega_t} v \cdot F \sqrt{1 + |\nabla h|^2} \, dx \, dy - \int_{\Omega_t} D \frac{e''(c)}{\sqrt{1 + |\nabla h|^2}} \nabla c \cdot M \nabla c \, dx \, dy \\
 &+ \int_{\partial\Omega_t} -e(c) \frac{|\nabla h|^2}{\sqrt{1 + |\nabla h|^2}} v_{\text{CL}} - ce'(c) \frac{1}{\sqrt{1 + |\nabla h|^2}} v_{\text{CL}} \, ds + \int_{\partial\Omega_t} e(c) \sqrt{1 + |\nabla h|^2} v_{\text{CL}} \, ds \\
 &= - \int_{\Omega_t} v \cdot F \sqrt{1 + |\nabla h|^2} \, dx \, dy - \int_{\Omega_t} D \frac{e''(c)}{\sqrt{1 + |\nabla h|^2}} \nabla c \cdot M \nabla c \, dx \, dy + \int_{\partial\Omega_t} \gamma(c) v_{\text{CL}} \frac{1}{\sqrt{1 + |\nabla h|^2}} \, ds.
 \end{aligned}$$

Therefore in the presence of concentration contribution of surfactant, the energy dissipation law becomes

$$\begin{aligned}
 (3.13) \quad & \frac{d}{dt} \int_{\Omega_t} e(c) \sqrt{1 + |\nabla h|^2} \, dx \, dy + (\gamma_{\text{SL}} - \gamma_{\text{SG}}) \int_{\Omega_t} \, dx \, dy \\
 &= - \int_{\Omega_t} v \cdot F \sqrt{1 + |\nabla h|^2} \, dx \, dy - \int_{\Omega_t} D \frac{e''(c)}{\sqrt{1 + |\nabla h|^2}} \nabla c \cdot M \nabla c \, dx \, dy - \int_{\partial\Omega_t} F_s v_{\text{CL}} \, ds,
 \end{aligned}$$

where  $F_s = -\gamma(c) \cos \theta_{\text{CL}} + \gamma_{\text{SG}} - \gamma_{\text{SL}}$  is the concentration-dependent unbalanced Young force.

### 3.4. Stokes flow for bulk fluids and governing equations derived by Onsager's principle.

Now using Onsager's principle, we give the derivations for the governing equations of the surfactant induced Marangoni flow inside the droplets coupled with moving contact lines.

First, we impose the non-penetration boundary condition for the bottom of the droplet

$$(3.14) \quad u \cdot n = 0 \quad \text{on } \Omega_t$$

and consider an incompressible fluid satisfying  $\nabla \cdot u = 0$  inside the droplet  $A_t$ .

Assume the velocity  $v$  of the capillary surface coincides with the velocity  $u$  of the bulk fluids. Given  $h(x, y, t)$  and  $c(x, y, t)$ , then the energy dissipation (3.13) for the surface energy becomes a

linear functional of  $u, v_{\text{CL}}$  given by

$$(3.15) \quad \dot{\mathcal{F}}(u, v_{\text{CL}}; h, c) = - \int_{\Omega_t} u \cdot F \sqrt{1 + |\nabla h|^2} \, dx \, dy - \int_{\Omega_t} D \frac{e''(c)}{\sqrt{1 + |\nabla h|^2}} \nabla c \cdot M \nabla c \, dx \, dy - \int_{\partial\Omega_t} F_s v_{\text{CL}} \, ds.$$

Second, given  $h(x, y, t)$  and  $c(x, y, t)$ , introduce the Rayleigh dissipation functional  $Q$

$$(3.16) \quad \begin{aligned} Q(u, v_{\text{CL}}; h, c) := & \frac{\mu}{4} \int_{A_t} (\nabla u + \nabla u^\top) : (\nabla u + \nabla u^\top) \, dV + \frac{D}{2} \int_{\Omega_t} \frac{e''(c)}{\sqrt{1 + |\nabla h|^2}} \nabla c \cdot M \nabla c \, dx \, dy \\ & + \frac{\mu}{2\alpha} \int_{\Omega_t} u^2 \, dx \, dy + \frac{\xi}{2} \int_{\partial\Omega_t} |v_{\text{CL}}|^2 \, ds, \end{aligned}$$

where  $\mu$  is the dynamics viscosity for the bulk fluids and  $\alpha$  is the slip length.

Given  $h(x, y, t)$  and  $c(x, y, t)$ , define Rayleighian as

$$(3.17) \quad \mathcal{R}(u, v_{\text{CL}}; h, c) := Q(u, v_{\text{CL}}; h, c) + \dot{\mathcal{F}}(u, v_{\text{CL}}; h, c).$$

Then based on Onsager's principle, we minimize  $\mathcal{R}(u, v_{\text{CL}}; h, c)$  w.r.t the velocity  $u, v_{\text{CL}}$ . This yields the following governing equations, which derivations are given in three steps below.

After incorporating the transport equation (3.1) for surfactant  $c$  and the no-flux boundary condition (3.10), the minimization of  $\mathcal{R}(u, v_{\text{CL}}; h, c)$  gives the governing equations

$$(3.18) \quad \begin{cases} \begin{cases} \nabla p = \mu \Delta u & \text{in } A_t, \\ \nabla \cdot u = 0 & \text{in } A_t, \\ \sigma n = F & \text{on } S_t, \\ \frac{\alpha}{\mu} \tau \cdot \sigma n + \tau \cdot u = 0, \quad u \cdot n = 0 & \text{on } \Omega_t, \end{cases} \\ \begin{cases} \partial_t h + u_1 \partial_x h + u_2 \partial_y h = u_3 & \text{on } \Omega_t, \\ h = 0 & \text{on } \partial\Omega_t \\ \xi v_{\text{CL}} = F_s & \text{on } \partial\Omega_t, \end{cases} \\ \begin{cases} \partial_t \left( c \sqrt{1 + |\nabla_{xy} h|^2} \right) + \nabla_{xy} \cdot \left( c \sqrt{1 + |\nabla_{xy} h|^2} \begin{pmatrix} u_1 \\ u_2 \end{pmatrix} \right) = D \nabla_{xy} \cdot \left( \frac{1}{\sqrt{1 + |\nabla_{xy} h|^2}} M \nabla_{xy} \right) c & \text{on } \Omega_t, \\ \nabla_{xy} c \cdot n_\ell = 0 & \text{on } \partial\Omega_t, \end{cases} \end{cases}$$

where  $u_1(x, y, t) = u_x(x, y, h(x, y, t), t)$ ,  $u_2(x, y, t) = u_y(x, y, h(x, y, t), t)$  and

$$\sigma = -pI + \mu(\nabla u + \nabla u^\top), \quad F = \gamma(c)Hn + \nabla_s \gamma(c), \quad F_s = -\gamma(c) \cos \theta_{\text{CL}} + \gamma_{\text{SG}} - \gamma_{\text{SL}}.$$

The first group of (3.18) is the stationary Stokes equation inside the droplet coupled with the traction boundary condition balanced with the total capillary force density  $F$  and Navier slip boundary condition at the bottom. The second group of (3.18) is the evolution of the capillary surface induced by the fluid velocity and the moving contact line as a linear response to the concentration-dependent unbalanced Young force  $F_s$ . The third group of (3.18) is the transport equation for the insoluble surfactant with the no-flux boundary condition on the contact line  $\partial\Omega_t$ . We particularly point out that the Dirichlet boundary condition  $h = 0$  on  $\partial\Omega_t$  is necessary [21] because “the projection of the capillary forces onto the vertical axis is balanced out by a force of reaction exerted by the solid” [5, p.18]. We refer to [25] for the wellposedness of this model for



the 2D single droplet without surfactant. We remark in the case  $\alpha \rightarrow 0$ , the Navier slip boundary condition in the first group of (3.18) is reduced to the nonslip boundary condition  $u = 0$  on  $\Omega_t$ . In this case, the Rayleigh dissipation functional becomes

$$(3.19) \quad Q = \frac{\mu}{4} \int_{A_t} (\nabla u + \nabla u^\top) : (\nabla u + \nabla u^\top) \, dV + \frac{D}{2} \int_{\Omega_t} \frac{e''(c)}{\sqrt{1 + |\nabla h|^2}} \nabla c \cdot M \nabla c \, dx \, dy + \frac{\xi}{2} \int_{\partial\Omega_t} |v_{\text{CL}}|^2 \, ds.$$

The derivations of the governing equations (3.18) can be summarized as the following three steps.

Step 1. To impose the incompressible condition, introduce the Lagrangian multiplier  $p$ . Then we take the first variation of  $\mathcal{R}$  with perturbations  $u + \varepsilon \tilde{u}, p + \varepsilon \tilde{p}$  that compact supported in the open set  $A_t$ ,

$$(3.20) \quad 0 = \left. \frac{d}{d\varepsilon} \right|_{\varepsilon=0} \left( \mathcal{R}(u + \varepsilon \tilde{u}, v_{\text{CL}}; h, c) - \int_{A_t} (p + \varepsilon \tilde{p}) \nabla \cdot (u + \tilde{u}) \right).$$

This implies the static Stokes equation inside  $A_t$

$$(3.21) \quad \begin{aligned} \nabla \cdot \sigma &= 0, \quad \nabla \cdot u = 0, \\ \sigma &= -pI + \mu(\nabla u + \nabla u^\top). \end{aligned}$$

Step 2. From the non-penetration boundary condition (3.14), we take the first variation of  $\mathcal{R}$  with perturbations  $u + \varepsilon \tilde{u}$  satisfying  $\tilde{u} \cdot n|_{z=0} = 0$ . Using (3.21),

$$(3.22) \quad \begin{aligned} 0 &= \left. \frac{d}{d\varepsilon} \right|_{\varepsilon=0} \mathcal{R}(u + \varepsilon \tilde{u}, v_{\text{CL}}; h, c) \\ &= \frac{\mu}{2} \int_{A_t} (\nabla u + \nabla u^\top) : (\nabla \tilde{u} + \nabla \tilde{u}^\top) \, dV + \frac{\mu}{\alpha} \int_{\Omega_t} u \cdot \tilde{u} \, dx \, dy - \int_{S_t} \tilde{u} \cdot F \, ds \\ &= \int_{A_t} \sigma : \nabla \tilde{u} \, dV + \frac{\mu}{\alpha} \int_{\Omega_t} u \cdot \tilde{u} \, dx \, dy - \int_{S_t} \tilde{u} \cdot F \, ds \\ &= \int_{\Omega_t} \tilde{u} \cdot (\sigma n + \frac{\mu}{\alpha} u) \, dx \, dy + \int_{S_t} \tilde{u} \cdot (\sigma n - F) \, ds. \end{aligned}$$

By the arbitrary of  $\tilde{u}$ , this implies the Navier slip boundary condition for the bottom part

$$(3.23) \quad \frac{\alpha}{\mu} \tau \cdot \sigma n + \tau \cdot u = 0 \quad \text{on } \Omega_t$$

and the traction boundary condition on the capillary surface

$$(3.24) \quad \sigma n = F \quad \text{on } S_t.$$

Step 3. Taking first variation of  $R$  w.r.t  $v_{\text{CL}} + \varepsilon \tilde{v}_{\text{CL}}$ , we obtain the contact line speed

$$(3.25) \quad \xi v_{\text{CL}} = F_s \quad \text{on } \partial\Omega_t.$$

Thus after incorporating the transport of the surfactant, we obtain the governing equations (3.18) of the surfactant induced Marangoni flow for droplets on a substrate. As a consequence, the energy dissipation law is

$$(3.26) \quad \dot{\mathcal{F}} = -2Q.$$

Now we explain Onsager's reciprocal relation for the linear response of  $u, v_{\text{CL}}$  to the two unbalanced forces  $F, F_s$ . Given  $c(x, y, t)$  and  $h(x, y, t)$ , define an operator

$$\mathcal{K} : L^2(S_t) \rightarrow L^2(S_t), \quad F \mapsto u|_{S_t}$$

such that  $u$  solves the Stokes equations with traction force  $F$  (first group in (3.18)). Then the velocity fields  $u, v_{\text{CL}}$  solved from the governing equation (3.18) satisfy the following linear response relations

$$(3.27) \quad \begin{aligned} u &= \mathcal{K}F && \text{on } S_t, \\ v_{\text{CL}} &= \frac{1}{\xi} F_s && \text{on } \partial\Omega_t. \end{aligned}$$

**Proposition 3.1.**  *$\mathcal{K}$  is a bijective and self-adjoint operator from  $L^2(S_t)$  onto  $L^2(S_t)$ .  $\mathcal{K}$  is a positive operator in  $L^2(S_t)$ . Further more, for the no-slip boundary condition case, i.e.,  $\alpha = 0$ , then  $\mathcal{K}$  is a bounded operator in  $L^2(S_t)$  satisfying*

$$(3.28) \quad \int_{S_t} F \cdot \mathcal{K}F \, ds \geq C \int_{S_t} |\mathcal{K}F|^2 \, ds \quad \text{for any } F \in L^2(S_t).$$

*Proof.* First, given any  $f \in L^2(S_t)$ , the solution to

$$(3.29) \quad \begin{cases} \nabla p = \mu \Delta u & \text{in } A_t, \\ \nabla \cdot u = 0 & \text{in } A_t, \\ u = f & \text{on } S_t, \\ \frac{\alpha}{\mu} \tau \cdot \sigma n + \tau \cdot u = 0, \quad u \cdot n = 0 & \text{on } \Omega_t, \end{cases}$$

exists uniquely. This gives a unique  $F = \sigma u$  and thus  $\mathcal{K}$  is bijective operator from  $L^2(S_t)$  onto  $L^2(S_t)$ .

Second, for any  $F_1, F_2 \in L^2(S_t)$ , let  $u_1 = \mathcal{K}F_1$  and  $u_2 = \mathcal{K}F_2$ . Then we have

$$(3.30) \quad \begin{aligned} \int_{S_t} F_1 \cdot \mathcal{K}F_2 \, ds &= \int_{S_t} \sigma_1 n \cdot u_2 \, ds \\ &= \frac{\mu}{2} \int_{A_t} (\nabla u_1 + \nabla u_1^\top) : (\nabla u_2 + \nabla u_2^\top) \, dV + \frac{\mu}{\alpha} \int_{\Omega_t} u_1 \cdot u_2 \, dx \, dy = \int_{S_t} \mathcal{K}F_1 \cdot F_2 \, ds, \end{aligned}$$

which, together with  $D(\mathcal{K}) = L^2(S_t)$ , shows  $\mathcal{K}$  is self-adjoint.

Third, the positivity of  $\mathcal{K}$  is directly from

$$(3.31) \quad \int_{S_t} F \cdot \mathcal{K}F \, ds \geq 0.$$

This equality holds if and only if  $F \equiv 0$  because  $u|_{\Omega_t} = 0$  implies the Korn's inequality [6, (3)]

$$(3.32) \quad \int_{A_t} |\nabla u|^2 \, dV \leq C \int_{A_t} |\nabla u + \nabla u^\top|^2 \, dV,$$

where  $C$  is a generic constant.

Fourth, in the case  $\alpha = 0$ . Combining the trace theorem, the standard Poincaré's inequality and Korn's inequality (3.32), we know

$$(3.33) \quad \int_{S_t} |u|^2 \, ds \leq C \int_{A_t} (|u|^2 + |\nabla u|^2) \, dV \leq C \int_{A_t} |\nabla u + \nabla u^\top|^2 \, dV.$$

This concludes (3.28). □

We remark in the geometric motion case, the first equation in (2.50) is the linear response relation  $u = \frac{1}{\beta}F$ . Then Proposition 3.1 tells us the Rayleigh dissipation functional  $Q$  in (3.19) for the viscous flow is stronger than the one defined in (2.47) for the geometric motion case.

*Remark 2.* We also remark under the non-penetration boundary condition  $u \cdot n = 0$  on the bottom of the droplet, the Navier slip boundary condition on a textured substrate  $w(x, y)$  becomes

$$(3.34) \quad \frac{\alpha}{\mu} \tau \cdot \sigma n + \tau \cdot u = 0 \quad \text{on } \partial A_t \cap \{z = w\},$$

which is equivalent to

$$(3.35) \quad \alpha(n \cdot \nabla)(\tau \cdot u) + \tau \cdot u = \alpha u \cdot (n \cdot \nabla \tau + n \cdot \nabla \tau) \quad \text{on } \partial A_t \cap \{z = w\}.$$

In the case  $w = 0$ , then the Navier slip boundary condition is simplified as

$$(3.36) \quad \tau \cdot u = \alpha \partial_z(\tau \cdot u) \quad \text{on } \Omega_t.$$

#### 4. ALGORITHMS BASED ON UNCONDITIONALLY STABLE EXPLICIT BOUNDARY UPDATES

In this section, we propose some numerical schemes for the droplet dynamics with the surfactant on the moving capillary surface. These mainly rely on decoupling the motion of the contact lines, the motion of the capillary surface, and the dynamics of the surfactant on the surface. Therefore, we will adapt the 1st/2nd order schemes developed in [11] for the pure geometric motion of single droplets and then incorporate the constantly changed dynamic surface tension  $\gamma(c)$  due to the dynamics of the surfactant.

To give a clear presentation, we describe numerical schemes for 2D droplets. For the 3D droplets, the construction of the arbitrary Lagrangian-Eulerian method for the moving grids need to be developed and will be left for the future study. Before this, we first derive the governing equations for 2D droplets laid by surfactant but placed on an inclined textured substrate. This is described by the motion of the capillary surface, the moving contact lines and the transport of the surfactant.

**4.1. Contact line dynamics and surfactant effect for 2D droplets on an inclined textured substrate.** Given an inclined textured solid substrate, we follow the convention for studying droplets on an inclined substrate and choose the Cartesian coordinate system built on an inclined plane with effective inclined angle  $\theta_0$  such that  $-\frac{\pi}{2} < \theta_0 < \frac{\pi}{2}$ , i.e.,  $(\tan \theta_0)x$  is the new  $x$ -axis we choose; see Fig 1 (b). With this Cartesian coordinate system, the textured substrate is described by a graph function  $w(x)$  and the droplet is then described by

$$(4.1) \quad A_t := \{(x, y); a(t) \leq x \leq b(t), w(x) \leq y \leq u(x, t) + w(x)\}.$$

The motion of this droplet is described by the relative height function of the capillary surface  $u(x, t) \geq 0$  and the partially wetting domain  $a(t) \leq x \leq b(t)$  with free boundaries  $a(t), b(t)$ .

With the new Cartesian coordinate system, the substrate  $w(x)$  and the total height  $h(x, t) := u(x, t) + w(x)$ , one can use the same lift-up method to derive the continuity equation for  $c(x, t), x \in (a(t), b(t))$ , i.e.

$$(4.2) \quad c_t - v_n \partial_x \left( c \frac{h_x}{\sqrt{1 + h_x^2}} \right) = D \partial_{ss} c, \quad \partial_s = \frac{1}{\sqrt{1 + h_x^2}} \partial_x.$$

This is equivalent to

$$(4.3) \quad \partial_t c - v_n c_x \frac{h_x}{\sqrt{1+h_x^2}} - v_n c H = D \partial_{ss} c, \quad H = \partial_x \left( \frac{h_x}{\sqrt{1+h_x^2}} \right) = \frac{h_{xx}}{(1+h_x^2)^{\frac{3}{2}}}$$

Notice the compatibility condition (2.34) on the contact line now changes to

$$(4.4) \quad h_t|_b = -\partial_x u|_b b', \quad h_t|_a = -\partial_x u|_a a'$$

due to  $u(x(t), t) = 0$  at  $x = a, b$ . We will derive the energy dissipation law and the governing equation for droplets placed on an inclined textured surface below.

**4.2. Dissipation law for the surface energy with a textured substrate.** Multiplying (4.2) by  $e'(c)\sqrt{1+h_x^2}$ , same derivations as (2.28) gives

$$(4.5) \quad \partial_t \left( e(c)\sqrt{1+h_x^2} \right) + \gamma(c)Hh_t - \partial_x \left( e(c)\frac{h_t h_x}{\sqrt{1+h_x^2}} \right) = D e'(c) \partial_{ss} c \sqrt{1+h_x^2}.$$

On one hand, integration of the left-hand-side of (4.5) gives

$$\begin{aligned} & \int_{a(t)}^{b(t)} \partial_t \left( e(c)\sqrt{1+h_x^2} \right) + \gamma(c)Hh_t \, dx - e(c)\frac{h_x h_t}{\sqrt{1+h_x^2}} \Big|_a^b \\ &= \frac{d}{dt} \int_{a(t)}^{b(t)} e(c)\sqrt{1+h_x^2} \, dx + \int_{a(t)}^{b(t)} \gamma(c)Hh_t \, dx - e(c)\frac{h_x h_t}{\sqrt{1+h_x^2}} \Big|_a^b - b'e(c)\sqrt{1+h_x^2}|_b + a'e(c)\sqrt{1+h_x^2}|_a \\ &= \frac{d}{dt} \int_{a(t)}^{b(t)} \left( e(c)\sqrt{1+h_x^2} \right) \, dx + \int_{a(t)}^{b(t)} \gamma(c)Hh_t \, dx - e(c)I_b + e(c)I_a, \end{aligned}$$

where we used the Reynolds transport theorem and

$$(4.6) \quad I_b := b'\sqrt{1+h_x^2}|_b + \frac{h_x h_t}{\sqrt{1+h_x^2}} \Big|_b, \quad I_a := a'\sqrt{1+h_x^2}|_a + \frac{h_x h_t}{\sqrt{1+h_x^2}} \Big|_a.$$

Then by compatibility condition (4.4),

$$(4.7) \quad I_b = b' \left( \sqrt{1+h_x^2} - \frac{h_x u_x}{\sqrt{1+h_x^2}} \right) = \frac{b'(1+h_x w_x)}{\sqrt{1+h_x^2}} \Big|_b, \quad I_a = \frac{a'(1+h_x w_x)}{\sqrt{1+h_x^2}} \Big|_a.$$

On the other hand, the right-hand-side of (4.5) becomes

$$\int_a^b D e'(c) \partial_x \left( \frac{c_x}{\sqrt{1+h_x^2}} \right) \, dx = -D \int_a^b e''(c) \frac{c_x^2}{\sqrt{1+h_x^2}} \, dx + D \frac{\partial_x e(c)}{\sqrt{1+h_x^2}} \Big|_a^b.$$

Therefore,

$$\begin{aligned} & \frac{d}{dt} \int_{a(t)}^{b(t)} \left( e(c)\sqrt{1+h_x^2} \right) \, dx + \int_{a(t)}^{b(t)} \gamma(c)h_t H \, dx + D \int_a^b e''(c) \frac{c_x^2}{\sqrt{1+h_x^2}} \, dx \\ (4.8) \quad &= e(c(b))I_b - e(c(a))I_a + D \frac{\partial_x e(c)}{\sqrt{1+h_x^2}} \Big|_a^b. \end{aligned}$$

Particularly for  $e(c) = c$ , we have

$$(4.9) \quad 0 = \frac{d}{dt} \int_{a(t)}^{b(t)} \left( c\sqrt{1+h_x^2} \right) \, dx = \cos \theta_b [Dc_x|_b + c(b)(1+h_x w_x)b'] - \cos \theta_a [Dc_x|_a + c(a)(1+h_x w_x)a'],$$

where  $\cos \theta_a = \frac{1}{\sqrt{1+h_x^2}}|_a$ ,  $\cos \theta_b = \frac{1}{\sqrt{1+h_x^2}}|_b$  and  $\theta_a, \theta_b$  are the dynamic contact angle at  $a, b$  respectively. Same as (2.39), to maintain the mass conservation law, we impose the Robin boundary condition for surfactant concentration (4.2)

$$(4.10) \quad Dc_x|_b + c(b)(1 + h_x w_x)|_b b' = 0, \quad Dc_x|_a + c(a)(1 + h_x w_x)|_a a' = 0.$$

Using boundary condition (4.10), we further simplify (4.8) as

$$(4.11) \quad \begin{aligned} & \frac{d}{dt} \int_{a(t)}^{b(t)} \left( e(c) \sqrt{1 + h_x^2} \right) dx + \int_{a(t)}^{b(t)} \gamma(c) h_t H dx + D \int_a^b e''(c) \frac{c_x^2}{\sqrt{1 + h_x^2}} dx \\ &= \cos \theta_b (e(c(b))(1 + h_x w_x)|_b b' + D e' c_x|_b) - \cos \theta_a (e(c(a))(1 + h_x w_x)|_a a' + D e' c_x|_a) \\ &= \cos \theta_b \gamma(c(b)) b' (1 + h_x w_x)|_b - \cos \theta_a \gamma(c(a)) a' (1 + h_x w_x)|_a. \end{aligned}$$

**4.3. The Onsager principle and the governing equations.** For a 2D droplet placed on an inclined textured surface, with the gravitational effect and the volume constraint  $V$ , we take the total free energy of the droplet as

$$(4.12) \quad \begin{aligned} \mathcal{F}(h(t), a(t), b(t), \lambda(t)) &= \int_{a(t)}^{b(t)} e(c) \sqrt{1 + (\partial_x h)^2} dx + (\gamma_{SL} - \gamma_{SG}) \int_{a(t)}^{b(t)} \sqrt{1 + (\partial_x w)^2} dx \\ &\quad + \rho g \int_{a(t)}^{b(t)} \int_w^{u+w} (y \cos \theta_0 + x \sin \theta_0) dy dx - \lambda(t) \left( \int_{a(t)}^{b(t)} u dx - V \right), \end{aligned}$$

where  $h = u + w$ ,  $e(c)$  is the energy density on the capillary surface,  $\rho$  is the density of the liquid, and  $g$  is the gravitational acceleration. Denote  $\kappa := \rho g$ .

Notice the time derivative of the second term in  $\mathcal{F}$  is

$$\frac{d}{dt} (\gamma_{SL} - \gamma_{SG}) \int_{a(t)}^{b(t)} \sqrt{1 + (\partial_x w)^2} dx = (\gamma_{SL} - \gamma_{SG}) (b' \sqrt{1 + (\partial_x w)^2}|_b - a' \sqrt{1 + (\partial_x w)^2}|_a),$$

and from  $u|_{a,b} = 0$ , the time derivative of the third term in  $\mathcal{F}$  is

$$(4.13) \quad \frac{d}{dt} \kappa \int_{a(t)}^{b(t)} \int_w^{u+w} (y \cos \theta_0 + x \sin \theta_0) dy dx = \kappa \int_{a(t)}^{b(t)} h_t (h \cos \theta_0 + x \sin \theta_0) dx.$$

This, together with the energy dissipation (4.11), gives

$$(4.14) \quad \begin{aligned} \frac{d}{dt} \mathcal{F} &= - \int_{a(t)}^{b(t)} (\gamma(c) H + \lambda - \kappa (h \cos \theta_0 + x \sin \theta_0) h_t) dx - D \int_{a(t)}^{b(t)} e''(c) \frac{c_x^2}{\sqrt{1 + h_x^2}} dx \\ &\quad + b' [\cos \theta_b \gamma(c(b))(1 + h_x w_x)|_b + (\gamma_{SL} - \gamma_{SG}) \sqrt{1 + (\partial_x w)^2}|_b] \\ &\quad - a' [\cos \theta_a \gamma(c(a))(1 + h_x w_x)|_a + (\gamma_{SL} - \gamma_{SG}) \sqrt{1 + (\partial_x w)^2}|_a]. \end{aligned}$$

Choose the Rayleigh dissipation functional as

$$(4.15) \quad Q := \frac{\beta}{2} \int_{a(t)}^{b(t)} \frac{h_t^2}{\sqrt{1 + h_x^2}} dx + \frac{\xi}{2} (|b'|^2 + |a'|^2) + \frac{D}{2} \int_{a(t)}^{b(t)} e''(c) \frac{c_x^2}{\sqrt{1 + h_x^2}} dx$$

Then by the same derivations as (2.48)-(2.50) for the 3D case, we conclude the governing equations for the full dynamics of a 2D single droplet on a textured substrate

$$(4.16) \quad \left\{ \begin{array}{l} \frac{\beta}{\sqrt{1+h_x^2}} h_t = \gamma(c)H - \kappa(h \cos \theta_0 + x \sin \theta_0) + \lambda, \quad \text{in } (a(t), b(t)) \\ (h-w)|_a = 0, \quad (h-w)|_b = 0, \\ c_t - v_n \partial_x \left( c \frac{h_x}{\sqrt{1+h_x^2}} \right) = D \partial_{ss} c, \quad \text{in } (a(t), b(t)) \\ Dc_x|_b + c(b)b'(1+h_x w_x)|_b = 0, \quad Dc_x|_a + c(a)a'(1+h_x w_x)|_a = 0, \\ \xi b' = -\cos \theta_b \gamma(c(b))(1+h_x w_x)|_b - (\gamma_{SL} - \gamma_{SG})\sqrt{1+(\partial_x w)^2}|_b, \\ \xi a' = \cos \theta_a \gamma(c(a))(1+h_x w_x)|_a + (\gamma_{SL} - \gamma_{SG})\sqrt{1+(\partial_x w)^2}|_a, \\ \int_{a(t)}^{b(t)} h \, dx = V, \end{array} \right.$$

where  $\partial_s = \frac{1}{\sqrt{1+h_x^2}} \partial_x$  and  $H = \partial_x \left( \frac{h_x}{\sqrt{1+h_x^2}} \right) = \frac{h_{xx}}{(1+h_x^2)^{\frac{3}{2}}}$  is the mean curvature. After taking into account the textured substrate, we remark that the unbalanced Young force becomes

$$(4.17) \quad F_b = -\cos \theta_b \gamma(c(b))(1+h_x w_x)|_b - (\gamma_{SL} - \gamma_{SG})\sqrt{1+(\partial_x w)^2}|_b,$$

$$(4.18) \quad F_a = \cos \theta_a \gamma(c(a))(1+h_x w_x)|_a + (\gamma_{SL} - \gamma_{SG})\sqrt{1+(\partial_x w)^2}|_a.$$

As a consequence, the energy dissipation relation (2.51) becomes

$$\frac{d}{dt} \mathcal{F} = -\beta \int_{a(t)}^{b(t)} \frac{h_t^2}{\sqrt{1+h_x^2}} \, dx - D \int_a^b e''(c) \frac{c_x^2}{\sqrt{1+h_x^2}} \, dx - \xi(|b'|^2 + |a'|^2) = -2Q.$$

Before proceeding to the computations for the full dynamics (4.16), we recast the equation (4.3) for the dynamics of surfactant concentration  $c$  as

$$(4.19) \quad c_t - \frac{h_t h_x}{1+h_x^2} c_x - \frac{h_t h_{xx}}{(1+h_x^2)^2} c = D \frac{c_{xx}}{1+h_x^2} - \frac{D h_x h_{xx}}{(1+h_x^2)^2} c_x,$$

which is a computationally friendly form.

**4.4. Numerical schemes.** We will split the PDE solver for the full dynamics of droplets with surfactant into the following three steps: (i) explicit boundary updates; (ii) semi-implicit capillary surface updates and (iii) implicit surfactant updates. The unconditional stability for the explicit 1D boundary updates is proved in [11], which efficiently decouples the computations of the boundary evolution and the capillary surface updates. The semi-implicit capillary surface updates with the volume constraint and the implicit surfactant updates can be convert to standard elliptic solvers at each step.

Let  $t^n = n\Delta t$ ,  $n = 0, 1, \dots$  with time step  $\Delta t$ . We approximate  $a(t^n), b(t^n), h(t^n)$  by  $a^n, b^n, h^n$  respectively. We present the first order scheme as follows. For completeness, we also provide a pseudo-code in Appendix B.

*First order scheme:*

Step 1. Explicit boundary updates. Compute the one-side approximated derivative of  $h^n$  at  $b^n$  and  $a^n$ , denoted as  $(\partial_x h^n)_N$  and  $(\partial_x h^n)_0$ . Then by the moving contact line boundary conditions in (4.16), we update  $a^{n+1}, b^{n+1}$  using

$$(4.20) \quad \begin{aligned} \xi \frac{a^{n+1} - a^n}{\Delta t} &= \cos \theta_a^n \gamma(c_0^n) (1 + (h_x^n)_0 (w_x)_0) + (\gamma_{SL} - \gamma_{SG}) \sqrt{1 + (\partial_x w)_0^2}, \quad \cos \theta_a^n = \frac{1}{\sqrt{1 + (h_x^n)_0^2}}, \\ \xi \frac{b^{n+1} - b^n}{\Delta t} &= -\cos \theta_b^n \gamma(c_N^n) (1 + (h_x^n)_N (w_x)_N) - (\gamma_{SL} - \gamma_{SG}) \sqrt{1 + (\partial_x w)_N^2}, \quad \cos \theta_b^n = \frac{1}{\sqrt{1 + (h_x^n)_N^2}}. \end{aligned}$$

Step 2. Rescale  $h^n$  from  $[a^n, b^n]$  to  $[a^{n+1}, b^{n+1}]$  with  $O(\Delta t^2)$  accuracy using an ALE discretization. For  $x^{n+1} \in [a^{n+1}, b^{n+1}]$ , denote the map from moving grids at  $t^{n+1}$  to  $t^n$  as

$$(4.21) \quad x^n := a^n + \frac{b^n - a^n}{b^{n+1} - a^{n+1}} (x^{n+1} - a^{n+1}) \in [a^n, b^n].$$

Define the rescaled solution for  $h^n$  as

$$(4.22) \quad h^{n*}(x^{n+1}) := h^n(x^n) + \partial_x h^n(x^n)(x^{n+1} - x^n).$$

By the Taylor expansion, it is easy to verify that  $h^{n*}(x^{n+1}) = h^n(x^{n+1}) + O(|x^n - x^{n+1}|^2)$ . From [11, (B.11)], we have the first order accuracy of

$$(4.23) \quad \partial_t h(x^{n+1}, t^{n+1}) = \frac{h(x^{n+1}, t^{n+1}) - h^{n*}(x^{n+1}, t^n)}{\Delta t} + O(\Delta t).$$

Step 3. Capillary surface updates with the volume constraint. Update  $h^{n+1}$  and  $\lambda^{n+1}$  semi-implicitly.

$$(4.24) \quad \begin{aligned} \frac{\beta}{\sqrt{1 + (\partial_x h^{n*})^2}} \frac{h^{n+1} - h^{n*}}{\Delta t} &= \frac{\gamma(c^n)}{(1 + (\partial_x h^{n*})^2)^{\frac{3}{2}}} \partial_{xx} h^{n+1} - \kappa(h^{n+1} \cos \theta_0 + x^{n+1} \sin \theta_0) + \lambda^{n+1}, \\ h^{n+1}(a^{n+1}) &= w(a^{n+1}), \quad h^{n+1}(b^{n+1}) = w(b^{n+1}), \\ \int_{a^{n+1}}^{b^{n+1}} u^{n+1}(x^{n+1}) \, dx^{n+1} &= \int_{a^0}^{b^0} u^0(x^0) \, dx^0, \end{aligned}$$

where the independent variable is  $x^{n+1} \in (a^{n+1}, b^{n+1})$ .

Step 4. Update the concentration of surfactant.

$$(4.25) \quad \begin{aligned} (h_t)^{n+1} &:= \frac{h^{n+1} - h^{n*}}{\Delta t}, \\ (1 + (h_x^{n+1})^2) \frac{c^{n+1} - c^n}{\Delta t} &= D \partial_{xx} c^{n+1} - \frac{D h_x^{n+1} h_{xx}^{n+1}}{1 + (h_x^{n+1})^2} \partial_x c^n + h_t^{n+1} h_x^{n+1} \partial_x c^n + \frac{h_t^{n+1} h_{xx}^{n+1}}{1 + (h_x^{n+1})^2} c^n \end{aligned}$$

with boundary conditions

$$(4.26) \quad \begin{aligned} D(c_x)_0^{n+1} + c_0^{n+1} (1 + (h_x)_0 (w_x)_0) \frac{a^{n+1} - a^n}{\Delta t} &= 0, \\ D(c_x)_N^{n+1} + c_N^{n+1} (1 + (h_x)_N (w_x)_N) \frac{b^{n+1} - b^n}{\Delta t} &= 0. \end{aligned}$$

We remark that the second order numerical scheme developed in [11] can be adapted here. When there are topological changes of droplets such as splitting and merging due to an impermeable

textured substrate, the projection method for solving variational inequalities developed in [12] can also be adapted.

## 5. COMPUTATIONS FOR DROPLETS WITH DYNAMIC SURFACE TENSION

We now use the numerical schemes in Section 4.4 to demonstrate several challenging examples: (i) the surface tension decreasing phenomena and asymmetric capillary surfaces due to the presence of the surfactant; (ii) the enhanced contact angle hysteresis or resistance with gravity for droplets placed on an inclined substrate; (iii) droplets on a textured substrate or in a container with different surfactant concentrations.

**5.1. Surface tension decreasing phenomena and asymmetric capillary surface due to the presence of surfactant.** In the first example, we compute the adhesion of a droplet placed on a flat plane to observe the surface tension decreasing phenomena due to the presence of different concentrations of surfactant.

First, we set the initial droplet as a spherical cap profile

$$(5.1) \quad h(x, 0) = \sqrt{R^2 - x^2} - R \cos(\theta_{\text{in}}) \quad \text{with } R = \frac{b_0}{\theta_{\text{in}}}, \quad b_0 = 3.7, \quad \theta_{\text{in}} = \frac{3\pi}{16}$$

and the computational parameters as follows

$$(5.2) \quad \beta = 0.1, \quad \kappa = 0.5, \quad \gamma_{\text{SL}} - \gamma_{\text{SG}} = -0.7, \quad \xi = 1; \quad D = 0.1; \quad T = 1.5; \quad \Delta t = 0.015, \quad N = 800.$$

Following (2.29), the concentration-dependent surface tension  $\gamma(c)$  is taken to be

$$(5.3) \quad \gamma(c) = \gamma_0 + \ln(1 - c) \quad \text{with } \gamma_0 = 2.$$

This means  $\gamma(c)$  is decreasing w.r.t  $c$  and if  $c = 0$ , the equilibrium Young's angle is given by  $\cos \theta_Y = -\frac{\gamma_{\text{SL}} - \gamma_{\text{SG}}}{\gamma_0} = 0.35$ .

In Fig. 2 (upper one), we first take  $c = 0$  and compute the adhering process without the surfactant starting from the initial droplet (5.1) to time  $T = 1.5$ . We observe the initial symmetric droplet (marked with black pentagrams) tends to shrink to its equilibrium symmetrically; see the symmetric droplet profile at  $T = 1.5$  (marked with black circles). Notice the dynamics of the concentration of surfactant  $c$  is shown on the capillary surface using different color; see color bar on the right side of the figures. The evolution of the capillary surface is drawn at equal time intervals with solid thin lines and patched with color showing the surfactant concentration.

Then in Fig. 2 (middle one), we take a uniform initial concentration of surfactant  $c(x, 0) = 0.8$  and start from the same initial symmetric droplet, which is marked with black pentagrams and is patched with a uniform color. We observe that, as time increases to  $T = 1.5$ , the droplet tends to spread out like a thin film due to the lower effective surface tension  $\gamma(c)$ ; see the flatten droplet profile at  $T = 1.5$  (marked with black circles). During the adhering process, the concentration of the surfactant at two contact endpoints decreases, so we observe the droplet still holds a pancake shape instead of completely spreading out; see similar droplet profiles in the lubrication model [28, 20].

To see the significant contribution of different surfactant concentrations to the droplet profile, we use the same initial capillary surface (marked with black pentagrams) but take an asymmetric



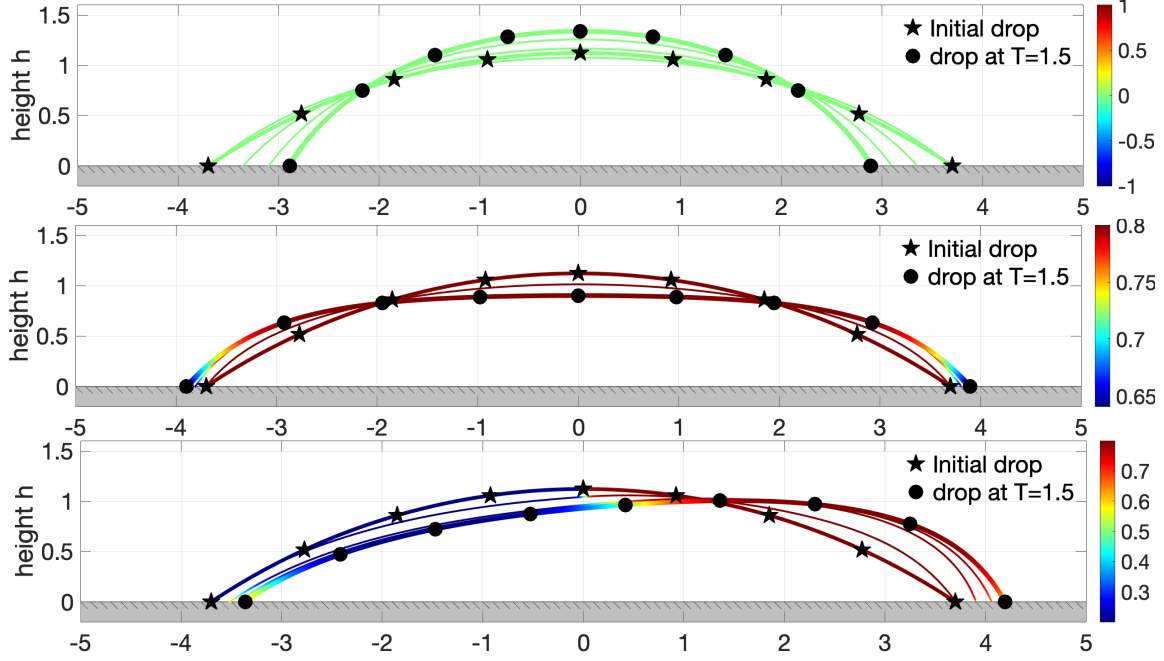


FIGURE 2. Adhesion of droplets on a plane with lower surface tension due to the surfactant effect. (upper) Time evolution of the capillary surface without the surfactant starting from an initial profile (5.1) marked with black pentagrams to a droplet profile marked with black circles at the final time  $T = 1.5$ . (middle) With initial concentration  $c = 0.8$ , the flattened droplet with a pancake shape is shown with a density-patched surface at  $T = 1.5$ . (lower) With an asymmetric initial concentration (5.4), an asymmetric evolution with the surfactant 'drag' effect is shown at equal time intervals and at  $T = 1.5$ .

initial concentration of the surfactant in Fig. 2 (lower one). Explicitly, we take initial concentration as

$$(5.4) \quad c(x, 0) = 0.5 + \frac{0.6}{\pi} \arctan(100x),$$

which increases from 0.2 to 0.8 with a sharp transition; see the patched curve marked with black pentagrams. Then as time increases, the surfactant 'drags' the droplet to the right and induces an asymmetric motion. We can observe an advancing contact angle and a receding contact angle in the droplet profile at  $T = 1.5$  (marked with black circles).

**5.2. Droplet on an inclined surface.** In the second example, we compute the adhesion of a droplet placed on an inclined substrate to observe the competition between the gravitational effect and the concentration-dependent capillary effect due to the presence of different concentration of the surfactant.

We use the same initial droplet profile (5.1) and take the inclined angle  $\theta_0 = 0.3$  for the substrate. We use the following computational parameters in Fig. 3

$$(5.5) \quad \beta = 0.1, \quad \kappa = 0.5, \quad \gamma_{SL} - \gamma_{SG} = -0.75, \quad \xi = 1, \quad D = 0.1, \quad \Delta t = 0.02, \quad N = 800.$$

Same as Fig. 2, the evolution of the capillary surface is drawn at equal time intervals with solid thin lines and patched with color showing surfactant concentration.

In Fig. 3 (upper one), we take  $c = 0$  and compute the evolution of a droplet without surfactant as a comparison. We can observe the contact angle hysteresis (CAH) in the droplet profile at  $T = 2$  (marked with black circles) with an advancing contact angle and a receding contact angle due to the gravity, which is unapparent.

However, in Fig. 3 (middle one), to see the enhanced CAH due to the surfactant effect, we take an asymmetric initial concentration

$$(5.6) \quad c(x, 0) = 0.45 - \frac{0.5}{\pi} \arctan(100x),$$

which decreases from 0.7 to 0.2 with a sharp transition; see the patched curve marked with black pentagrams in Fig. 3 (middle one). As time increases, we see the gravity and the asymmetric concentration of the surfactant (left part higher than the right part of the capillary surface) accelerate the rolling down of the droplet. Then droplet profile at  $T = 2$  is marked with black circles and patched with the surfactant concentration, in which we observe a significant enhancement of CAH phenomena with very different advancing contact angles and receding contact angles. On the other hand, if we switch the initial concentration of the surfactant to

$$(5.7) \quad c(x, 0) = 0.45 + \frac{0.5}{\pi} \arctan(100x)$$

so that the right part has higher concentration than the left part of the capillary surface. Then in Fig. 3 (lower one), we observe the surfactant effect wins the competition with the gravity and the droplet even rises up instead of rolling down; see the droplet profile at  $T = 2$  (marked with black circles).

**5.3. Droplets on a textured substrate and in a cocktail glass.** In the third example, we compute the adhesion of a droplet on some typical textured substrates such as a cocktail glass and a substrate with constantly changed effective slope. The common computational parameters are

$$(5.8) \quad \beta = 0.1, \quad \kappa = 0.5, \quad \xi = 1; \quad D = 0.5; \quad \Delta t = 0.02.$$

In Fig. 4 (upper), we take the initial droplet profile (marked with black pentagrams) as

$$(5.9) \quad h(x, 0) = \sqrt{R^2 - x^2} - R \cos(\theta_{\text{in}}) + w(b_0) + \frac{[w(b_0) - w(-b_0)](x + b_0)}{2b_0}, \quad R = \frac{b_0}{\theta_{\text{in}}}, \quad b_0 = 3.7$$

with  $\theta_{\text{in}} = \frac{3\pi}{16}$  and a cocktail glass substrate

$$(5.10) \quad w(x) = 0.5\sqrt{x^2 + 0.1}.$$

Then taking  $\gamma_{\text{SL}} - \gamma_{\text{SG}} = -0.9$ ,  $N = 1600$  and the initial concentration of the surfactant as  $c(x, 0) = 0.2$ , time evolution of the density-patched capillary surfaces is shown at equal time intervals and at the final time  $T = 4$  (marked with black circles). We observe the capillary rise near the contact lines and the surfactant tends to push themselves and concentrate near the contact lines.

In Fig. 4 (lower), we take the initial droplet profile (marked with black pentagrams) as (5.9) with  $\theta_{\text{in}} = \frac{1.3\pi}{8}$ , an effective inclined angle  $\theta_0 = 0.2$  and a textured substrate

$$(5.11) \quad w(x) = 0.1 (\sin(2x) + \cos(4x))^2.$$

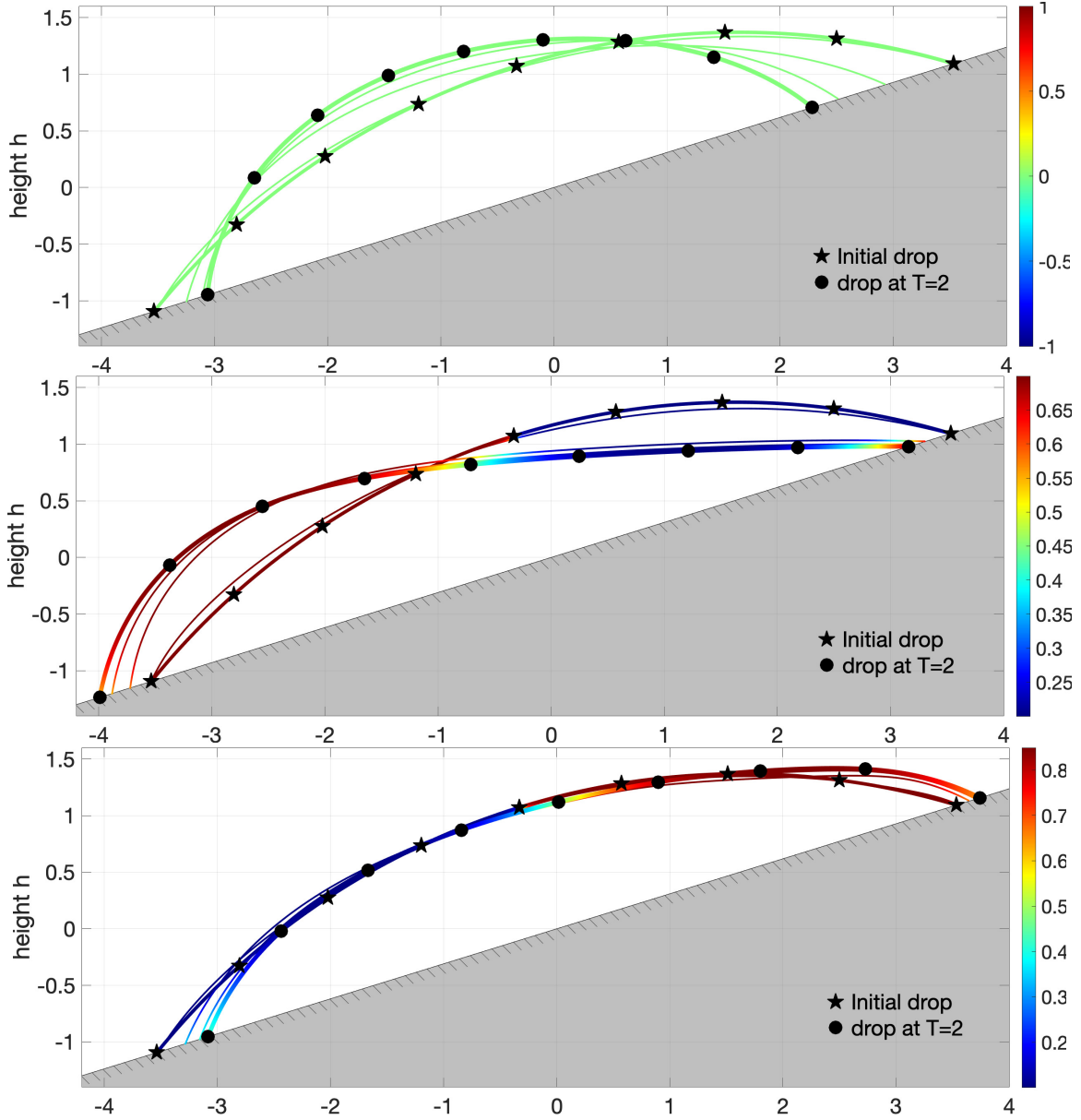


FIGURE 3. Enhanced CAH and resistance with the gravity due to asymmetric concentration of surfactant for a droplet placed on an inclined substrate with  $\theta_0 = 0.3$ . (upper) Time evolution of the capillary surface without the surfactant starting from an initial profile (5.1) marked with black pentagrams to a droplet profile marked with black circles at a final time  $T = 2$ . (middle) With the initial concentration (5.6), the significant enhancement of rolling down and the CAH phenomena are shown with density-patched surfaces at equal time intervals and at  $T = 2$ . (lower) With the initial concentration (5.7), the droplet rises up instead of rolling down because the surfactant effect wins the competition with the gravity.

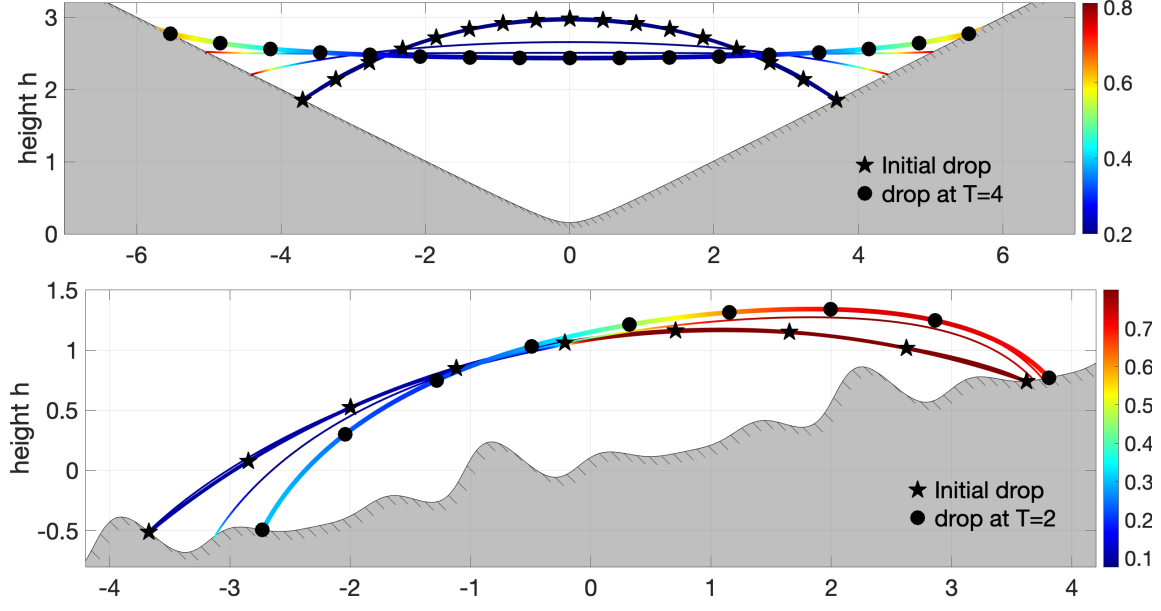


FIGURE 4. The upper figure is the time evolution of a droplet in a cocktail glass with a uniform initial concentration of surfactant. The initial profile (5.9) is marked with black pentagrams while the density-patched capillary surface at the final time  $T = 4$  is marked with black circles. The lower figure is the time evolution of a droplet on a inclined textured substrate (5.11). An asymmetric rising up starting from (5.12) is shown with the density-patched capillary surfaces at equal time intervals and at  $T = 2$ .

Then taking  $\gamma_{SL} - \gamma_{SG} = -0.5$ ,  $N = 800$  and the initial asymmetric concentration of the surfactant as

$$(5.12) \quad c(x, 0) = 0.45 + \frac{0.7}{\pi} \arctan(100x),$$

time evolution of the density-patched capillary surfaces is shown at equal time intervals and at final time  $T = 2$  (marked with black circles). We observe an asymmetric rising up of the droplet due to the asymmetric initial concentration and the constantly changed effective slope of the textured substrate.

#### APPENDIX A. PROOF OF PROPOSITION 2.1

*Proof of Proposition 2.1.* Recall the continuity equation (2.9) on wetting domain  $\Omega_t$  and the relation (2.15) between  $c$  and  $\mathcal{C}$ . We then have

$$\begin{aligned} 0 &= \partial_t \left( c \sqrt{1 + |\nabla h|^2} \right) + \nabla \cdot \left( c \sqrt{1 + |\nabla h|^2} v_{xy} \right) \\ (A.1) \quad &= \sqrt{1 + |\nabla h|^2} \left( (\partial_t + v_{xy} \cdot \nabla_{xy}) c \right) + c \left( \partial_t \sqrt{1 + |\nabla h|^2} + \nabla_{xy} \cdot \left( \sqrt{1 + |\nabla h|^2} v_{xy} \right) \right) \\ &= \sqrt{1 + |\nabla h|^2} \left( (\partial_t + v \cdot \nabla) \mathcal{C} \right) + \mathcal{C} \left( \partial_t \sqrt{1 + |\nabla h|^2} + \nabla_{xy} \cdot \left( \sqrt{1 + |\nabla h|^2} v_{xy} \right) \right) \end{aligned}$$

where  $v_{xy} := \begin{pmatrix} v_1 \\ v_2 \end{pmatrix} = \begin{pmatrix} \frac{-h_t h_x}{1 + |\nabla h|^2} \\ \frac{-h_t h_y}{1 + |\nabla h|^2} \end{pmatrix} + \begin{pmatrix} f \\ g \end{pmatrix}$  due to (2.7).

First, for the last term in (A.1), using the identity (2.27), we have

$$(A.2) \quad \partial_t \sqrt{1 + |\nabla h|^2} + \nabla_{xy} \cdot \left( \sqrt{1 + |\nabla h|^2} v_{xy} \right) = -h_t H + \nabla_{xy} \cdot \left( \sqrt{1 + |\nabla h|^2} \begin{pmatrix} f \\ g \end{pmatrix} \right)$$

This, together with (A.1), gives the equation for  $\mathcal{C}$

$$(A.3) \quad ((\partial_t + v \cdot \nabla) \mathcal{C}) - \mathcal{C} v_n H + \frac{1}{\sqrt{1 + |\nabla h|^2}} \nabla_{xy} \cdot \left( \sqrt{1 + |\nabla h|^2} \begin{pmatrix} f \\ g \end{pmatrix} \right) = 0.$$

Second, we prove the following claim

$$(A.4) \quad \nabla_s \cdot v_s = \frac{1}{\sqrt{1 + |\nabla h|^2}} \nabla_{xy} \cdot \left( \sqrt{1 + |\nabla h|^2} \begin{pmatrix} f \\ g \end{pmatrix} \right) = \partial_x f + \partial_y g + \frac{1}{2} \begin{pmatrix} f \\ g \end{pmatrix} \cdot \frac{\nabla_{xy}(|\nabla h|^2)}{1 + |\nabla h|^2}.$$

Denote

$$\tilde{f}(x, y, h(x, y, t)) = f(x, y, t), \quad \tilde{g}(x, y, h(x, y, t)).$$

Then for the tangential velocity

$$(A.5) \quad v_s = f \tau_1 + g \tau_2 = \begin{pmatrix} \tilde{f} \\ \tilde{g} \\ h_x \tilde{f} + h_y \tilde{g} \end{pmatrix},$$

by the chain rule, we have

$$(A.6) \quad \nabla \cdot v_s = \partial_x f + \partial_y g.$$

On the other hand,

$$(A.7) \quad \begin{aligned} -n(n \cdot \nabla) v_s &= -\frac{1}{1 + |\nabla h|^2} \begin{pmatrix} -h_x \\ -h_y \\ 1 \end{pmatrix} \cdot (-h_x \partial_x - h_y \partial_y + \partial_z) \begin{pmatrix} \tilde{f} \\ \tilde{g} \\ h_x \tilde{f} + h_y \tilde{g} \end{pmatrix} \\ &= \frac{1}{1 + |\nabla h|^2} (f(h_{xx} + h_{xy}) + g(h_{xy} + h_{yy})) = \frac{1}{2} \begin{pmatrix} f \\ g \end{pmatrix} \cdot \frac{\nabla_{xy}(|\nabla h|^2)}{1 + |\nabla h|^2}. \end{aligned}$$

Combining (A.6) and (A.7) yields (A.4).  $\square$

## APPENDIX B. PSEUDO-CODE FOR FIRST ORDER SCHEME

Below, we present a pseudo-code for the first order scheme in Section 4.4.

1. Grid for time:  $t^n = n\Delta t$ ,  $n = 0, 1, \dots$ , where  $\Delta t$  is time step.
2. Fix  $N$  and set moving grids for space:  $x_j^n = a^n + j\tau^n$ ,  $\tau^n = \frac{b^n - a^n}{N}$ ,  $j = -1, 0, 1, \dots, N + 1$ .
3. Calculate volume  $V := \sum_{j=1}^{N-1} (h^0 - w)(x_j^0) \tau^0$ .
4. Denote the finite difference operators

$$(B.1) \quad \begin{aligned} (\partial_x h)_0^n &= \frac{4h_1^n - h_2^n - 3h_0^n}{2\tau^n}, \quad (\partial_x h)_N^n = \frac{-4h_{N-1}^n + h_{N-2}^n + 3h_N^n}{2\tau^n}, \\ (\partial_x h)_j^n &= \frac{h_{j+1}^n - h_{j-1}^n}{2\tau^n}, \quad (\partial_{xx} h)_j^n = \frac{h_{j+1}^n - 2h_j^n + h_{j-1}^n}{(\tau^n)^2}, \quad j = 1, \dots, N-1. \end{aligned}$$

Denote

$$(\partial_x w)_0 := \partial_x w(x_0^n), \quad (\partial_x w)_N := \partial_x w(x_N^n), \quad \gamma_i^n := \gamma(c_i^n), \quad i = 0, \dots, N.$$

5. Update  $a^{n+1}, b^{n+1}, j = 0, 1, \dots, N$ ,

$$\begin{aligned}\xi \frac{a^{n+1} - a^n}{\Delta t} &= \gamma_0^n \frac{1 + (\partial_x h^n)_0 (\partial_x w)_0}{\sqrt{1 + (\partial_x h^n)_0^2}} + (\gamma_{\text{SL}} - \gamma_{\text{SG}}) \sqrt{1 + (\partial_x w)_0^2}, \\ \xi \frac{b^{n+1} - b^n}{\Delta t} &= -\gamma_N^n \frac{1 + (\partial_x h^n)_N (\partial_x w)_N}{\sqrt{1 + (\partial_x h^n)_N^2}} - (\gamma_{\text{SL}} - \gamma_{\text{SG}}) \sqrt{1 + (\partial_x w)_N^2}.\end{aligned}$$

6. Update the moving grids  $x_j^{n+1} = a^{n+1} + j\tau^{n+1}$ ,  $\tau^{n+1} = \frac{b^{n+1} - a^{n+1}}{N}$ ,  $j = 0, 1, \dots, N$ .

7. From (4.22),  $h_j^{n*} = h_j^n + (\partial_x h^n)_j (a^{n+1} - a^n + j(\tau^{n+1} - \tau^n))$ ,  $j = 0, \dots, N$ .

8. Solve  $h^{n+1}$  semi-implicitly

For  $j = 1, \dots, N-1$ , denote  $\alpha_j = 1 + (h_x^2)_j^n$  and solve

$$\begin{aligned}\text{(B.2)} \quad \beta \alpha_j \frac{h_j^{n+1} - h_j^{n*}}{\Delta t} &= \gamma_j^n \frac{h_{j+1}^{n+1} - 2h_j^{n+1} + h_{j-1}^{n+1}}{(\tau^{n+1})^2} - \kappa \alpha_j^{3/2} (h_j^{n+1} \cos \theta_0 + x_j^{n+1} \sin \theta_0) + \lambda^{n+1} \alpha_j^{3/2}, \\ \sum_{j=1}^{N-1} (h_j^{n+1} - w(x_j^{n+1})) \tau^{n+1} &= V,\end{aligned}$$

with the Dirichlet boundary condition  $h_0^{n+1} = w(x_0^{n+1})$ ,  $h_N^{n+1} = w(x_N^{n+1})$ .

Denote a positive-definite matrix  $A_{(N-1) \times (N-1)} = (a_{ij})$  with

$$\text{(B.3)} \quad a_{j,j-1} := -\gamma_j^n, \quad a_{j,j+1} := -\gamma_j^n, \quad a_{j,j} := 2\gamma_j^n + \frac{\beta(\tau^{n+1})^2}{\Delta t} \alpha_j + \kappa \cos \theta_0 (\tau^{n+1})^2 \alpha_j^{\frac{3}{2}}$$

and a vector of length  $N-1$

$$\tilde{f}_j := \frac{\beta(\tau^{n+1})^2}{\Delta t} h_j^{n*} \alpha_j - \kappa \sin \theta_0 x_j^{n+1} (\tau^{n+1})^2 \alpha_j^{\frac{3}{2}}, \quad j = 1, \dots, N-1$$

and (B.2) becomes for  $j = 1, \dots, N-1$ ,

$$\text{(B.4)} \quad a_{j,j-1} h_{j-1}^{n+1} + a_{j,j} h_j^{n+1} + a_{j,j+1} h_{j+1}^{n+1} - \alpha_j^{\frac{3}{2}} (\tau^{n+1})^2 \lambda^{n+1} = \tilde{f}_j.$$

Denote

(B.5)

$$f_1 = \tilde{f}_1 + \gamma_1^n w(x_0^{n+1}), \quad \{f_j = \tilde{f}_j\}_{j=2}^{N-2}, \quad f_{N-1} = \tilde{f}_{N-1} + \gamma_{N-1}^n w(x_N^{n+1}), \quad f_N := \sum_{j=1}^{N-1} w(x_j^{n+1}) + \frac{V}{\tau^{n+1}}.$$

The resulting linear system  $\bar{A}y = f$  has a non-singular matrix

$$\text{(B.6)} \quad \bar{A} = \begin{pmatrix} A & \alpha^{\frac{3}{2}} \\ e^\top & 0 \end{pmatrix}_{N \times N},$$

where  $y^\top = (h_1^{n+1}, \dots, h_{N-1}^{n+1}, -(\tau^{n+1})^2 \lambda^{n+1})$  and  $e^\top = (1, \dots, 1) \in \mathbb{R}^{N-1}$ .

9. Solve  $c^{n+1}$  from (4.25) implicitly.

Denote

$$\begin{aligned}(h_t)_j^{n+1} &:= \frac{h_j^{n+1} - h_j^{n*}}{\Delta t}, \quad j = 1, \dots, N-1, \\ \tilde{f}_j &:= -D \frac{(h_x)_j^{n+1} (h_{xx})_j^{n+1}}{1 + (h_x^2)_j^{n+1}} (c_x)_j^n + (h_t)_j^{n+1} (h_x)_j^{n+1} (c_x)_j^n + \frac{(h_t)_j^{n+1} (h_{xx})_j^{n+1}}{1 + (h_x^2)_j^{n+1}} c_j^n.\end{aligned}$$

Then (4.25) becomes

$$(B.7) \quad (1 + (h_x^2)_j^{n+1}) \frac{c_j^{n+1} - c_j^n}{\Delta t} = D \frac{c_{j+1}^{n+1} - 2c_j^{n+1} + c_{j-1}^{n+1}}{(\tau^{n+1})^2} + \tilde{f}_j, \quad j = 1, \dots, N-1$$

with boundary conditions

$$(B.8) \quad \begin{aligned} D(c_x)_0^{n+1} + c_0^{n+1}(1 + (h_x)_0(w_x)_0) \frac{a^{n+1} - a^n}{\Delta t} &= 0, \\ D(c_x)_N^{n+1} + c_N^{n+1}(1 + (h_x)_N(w_x)_N) \frac{b^{n+1} - b^n}{\Delta t} &= 0, \end{aligned}$$

where

$$(\partial_x c)_0^{n+1} = \frac{4c_1^{n+1} - c_2^{n+1} - 3c_0^{n+1}}{2\tau^{n+1}}, \quad (\partial_x c)_N^{n+1} = \frac{-4c_{N-1}^{n+1} + c_{N-2}^{n+1} + 3c_N^{n+1}}{2\tau^{n+1}}.$$

Let

$$\iota_0 := \frac{2\tau^{n+1}}{D}(1 + (h_x)_0(w_x)_0) \frac{a^{n+1} - a^n}{\Delta t}, \quad \iota_N := \frac{2\tau^{n+1}}{D}(1 + (h_x)_N(w_x)_N) \frac{b^{n+1} - b^n}{\Delta t},$$

then boundary condition (B.8) becomes

$$(\iota_0 - 3)c_0^{n+1} + 4c_1^{n+1} - c_2^{n+1} = 0, \quad c_{N-2}^{n+1} - 4c_{N-1}^{n+1} + (\iota_N + 3)c_N^{n+1} = 0.$$

Now we recast (B.7) in a  $N + 1$  order matrix form

$$Bc^{n+1} = f, \quad B = (b_{ij})_{i,j=0,\dots,N}$$

where, for  $i = 0$ ,

$$b_{00} = \iota_0 - 3, \quad b_{01} = 4, \quad b_{02} = -1,$$

for  $i = 1, \dots, N-1$ ,

$$b_{i,i-1} = -1, \quad b_{i,i} = 2 + \frac{(\tau^{n+1})^2}{D\Delta t}(1 + (h_x^2)_i^{n+1}), \quad b_{i,i+1} = -1,$$

for  $i = N$ ,

$$b_{N,N-2} = 1, b_{N,N-1} = -4, b_{N,N} = \iota_N + 3$$

$$\text{and } f_0 = 0, f_N = 0, f_i = \frac{(\tau^{n+1})^2}{D} \left( \tilde{f}_i + \frac{1 + (h_x^2)_i^{n+1}}{\Delta t} c_i^n \right), \quad i = 1, \dots, N-1.$$

#### ACKNOWLEDGMENTS

The authors would like to thank Prof. Masao Doi and Prof. Tom Witelski for some helpful suggestions. J.-G. Liu was supported in part by the National Science Foundation (NSF) under award DMS-1812573.

## REFERENCES

- [1] P. Cermelli, E. Fried, and M. Gurtin. Transport relations for surface integrals arising in the formulation of balance laws for evolving fluid interfaces. *Journal of Fluid Mechanics*, 544:339–351, 2005.
- [2] K.-Y. Chen and M.-C. Lai. A conservative scheme for solving coupled surface-bulk convection–diffusion equations with an application to interfacial flows with soluble surfactant. *Journal of Computational Physics*, 257:1–18, 2014.
- [3] W.-L. Chou, P.-Y. Lee, C.-L. Yang, W.-Y. Huang, and Y.-S. Lin. Recent advances in applications of droplet microfluidics. *Micromachines*, 6(9):1249–1271, 2015.
- [4] P. G. de Gennes. Wetting: statics and dynamics. *Reviews of Modern Physics*, 57(3):827–863, Jul 1985.
- [5] P.-G. De Gennes, F. Brochard-Wyart, and D. Quéré. *Capillarity and wetting phenomena: drops, bubbles, pearls, waves*. Springer Science & Business Media, 2013.
- [6] L. Desvillettes and C. Villani. On a variant of korn’s inequality arising in statistical mechanics. *ESAIM: Control, Optimisation and Calculus of Variations*, 8:603–619, 2002.
- [7] M. Doi. *Soft matter physics*. Oxford University Press, first edition edition, 2013.
- [8] M. Doi. Onsager principle in polymer dynamics. *Progress in Polymer Science*, 112:101339, Jan 2021.
- [9] S. Ganesan. Simulations of impinging droplets with surfactant-dependent dynamic contact angle. *Journal of Computational Physics*, 301:178–200, Nov 2015.
- [10] Y. Gao, H. Ji, J.-G. Liu, and T. P. Witelski. Global existence of solutions to a tear film model with locally elevated evaporation rates. *Physica D: Nonlinear Phenomena*, 350:13–25, 2017.
- [11] Y. Gao and J.-G. Liu. Gradient flow formulation and second order numerical method for motion by mean curvature and contact line dynamics on rough surface. *to appear in Interfaces and Free boundaries*, 2020.
- [12] Y. Gao and J.-G. Liu. Projection method for droplet dynamics on groove-textured surface with merging and splitting. *arXiv preprint arXiv:2005.07851*, 2020.
- [13] H. Garcke and S. Wietland. Surfactant spreading on thin viscous films: Nonnegative solutions of a coupled degenerate system. *SIAM Journal on Mathematical Analysis*, 37(6):2025–2048, Jan 2006.
- [14] N. Grunewald and I. Kim. A variational approach to a quasi-static droplet model. *Calculus of Variations and Partial Differential Equations*, 41(1–2):1–19, May 2011.
- [15] M. E. Gurtin. *Configurational forces as basic concepts of continuum physics*, volume 137. Springer Science & Business Media, 1999.
- [16] G. Karapetsas, R. V. Craster, and O. K. Matar. On surfactant-enhanced spreading and superspreading of liquid drops on solid surfaces. *Journal of Fluid Mechanics*, 670:5–37, Mar 2011.
- [17] G. Karapetsas, K. C. Sahu, and O. K. Matar. Evaporation of sessile droplets laden with particles and insoluble surfactants. *Langmuir*, 32(27):6871–6881, Jul 2016.
- [18] M.-C. Lai. Numerical simulation of moving contact lines with surfactant by immersed boundary method. *Communications in Computational Physics*, 8(4):735–757, Jun 2010.
- [19] M.-C. Lai, Y.-H. Tseng, and H. Huang. An immersed boundary method for interfacial flows with insoluble surfactant. *Journal of Computational Physics*, 227(15):7279–7293, 2008.
- [20] L. Limat and H. Stone. Three-dimensional lubrication model of a contact line corner singularity. *EPL (Europhysics Letters)*, 65(3):365, 2004.
- [21] A. Marchand, J. H. Weijers, J. H. Snoeijer, and B. Andreotti. Why is surface tension a force parallel to the interface? *American Journal of Physics*, 79(10):999–1008, 2011.
- [22] A. A. Olajire. Review of aspeor (alkaline surfactant polymer enhanced oil recovery) technology in the petroleum industry: Prospects and challenges. *Energy*, 77:963–982, 2014.
- [23] N. Shembekar, C. Chaipan, R. Utharala, and C. A. Merten. Droplet-based microfluidics in drug discovery, transcriptomics and high-throughput molecular genetics. *Lab on a Chip*, 16(8):1314–1331, 2016.
- [24] H. A. Stone. A simple derivation of the time-dependent convective-diffusion equation for surfactant transport along a deforming interface. *Physics of Fluids A: Fluid Dynamics*, 2(1):111–112, Jan 1990.
- [25] I. Tice and L. Wu. Dynamics and stability of sessile drops with contact points. *Journal of Differential Equations*, 272:648 – 731, 2021.



- [26] M. Wu, Y. Di, X. Man, and M. Doi. Drying droplets with soluble surfactants. *Langmuir*, 35(45):14734–14741, 2019.
- [27] J.-J. Xu and W. Ren. A level-set method for two-phase flows with moving contact line and insoluble surfactant. *Journal of Computational Physics*, 263:71–90, 2014.
- [28] X. Xu, Y. Di, and M. Doi. Variational method for contact line problems in sliding liquids. *Phys. Fluids*, 28:087101, 2016.
- [29] Z. Zhang and W. Ren. Simulation of moving contact lines in two-phase polymeric fluids. *Computers & Mathematics with Applications*, 72(4):1002–1012, Aug 2016.
- [30] Z. Zhang, S. Xu, and W. Ren. Derivation of a continuum model and the energy law for moving contact lines with insoluble surfactants. *Physics of Fluids*, 26(6):062103, Jun 2014.